



Copernicus Climate Change Service



Description and user guide of the Worldwide CORDEX C3S dataset assessing potential conflicts due to overlaps

Issued by: IFCA-CSIC

Date: 22/09/2021

Ref: C3S_34d1.5.2-User_Guide_v2

Official reference number service contract: 2019/C3S_34d_CSIC-IFCA/

This document has been produced in the context of the Copernicus Climate Change Service (C3S).

The activities leading to these results have been contracted by the European Centre for Medium-Range Weather Forecasts, operator of C3S on behalf of the European Union (Delegation Agreement signed on 11/11/2014). All information in this document is provided "as is" and no guarantee or warranty is given that the information is fit for any particular purpose.

The user thereof uses the information at its sole risk and liability. For the avoidance of all doubts, the European Commission and the European Centre for Medium-Range Weather Forecasts has no liability in respect of this document, which is merely representing the authors view.





Contributors

CSIC-IFCA

Javier Díez
José M. Gutiérrez
Maialen Iturbide
Jesús Fernández

IPSL-CNRS

Guillaume Levavasseur

SMHI

Grigory Nikulin

Predictia

Daniel San Martín
Max Tuni



Table of Contents

1. Introduction	4
2. Description of the worldwide CORDEX dataset	4
2.1. The sub-ensemble CORDEX-CORE	7
3. Description of the participant RCMs (model metadata)	8
4. Assessment of regional overlaps	8
5. Using the CDS Toolbox: Some common problems and solutions	14
5.1. Spatial subsetting	16
5.2. Zonal and meridional averaging	17
5.3. Model intercomparison and/or evaluation	17
5.4. Polar regions	17
5.5. Plotting	17
5.6. Common python workflow using CDSAPI, Xarray, Numpy, Cartopy, Matplotlib	18
6. Conclusions	20
Annex. Metadata from the RCMs forming the dataset	21

1. Introduction

The main objective of the C3S_34d contract was producing a quality assured dataset of regional climate change projections gathering the simulations produced by the CORDEX¹ community worldwide (in addition to the European and Mediterranean data supplied by C3S_34b Lot 1 & 2). The dataset resulting from this contract has been published at the CDS together with C3S_34b results forming the catalogue “CORDEX regional climate model data on single levels”². It has become an authoritative dataset that is cross-referenced in other initiatives, such as the IPCC Sixth Assessment Report

The present document describes the final dataset and provides some user guidance on its use, in particular focusing on the consistency of simulations in overlapping areas and on the use of the CDS Toolbox to work with this dataset.

2. Description of the worldwide CORDEX dataset

The worldwide CORDEX dataset provided by this contract comprises regional climate projections from all CORDEX domains (<https://cordex.org/domains>, see Figure 1) except EURO-CORDEX and Med-CORDEX, which are supplied to the CDS through C3S_34b contracts (shown in red in Figure 1).

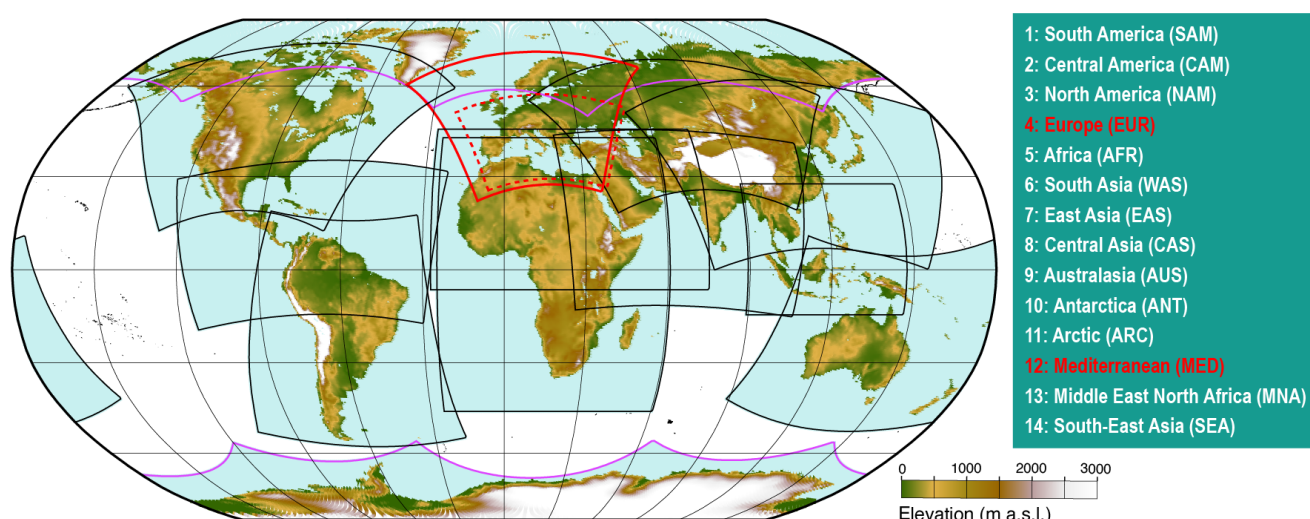


Figure 1. Fourteen official domains of the CORDEX initiative showing the model elevation corresponding to the standard 0.44° resolution.

The information of this contract was gathered both from the standardized ESGF repository and from local providers (the contract supported modeling centers for standardizing and publishing their data

¹ Gutowski et al., 2016; <https://doi.org/10.5194/gmd-9-4087-2016>

² <https://cds.climate.copernicus.eu/cdsapp#!/dataset/projections-cordex-domains-single-levels>



into ESGF). Therefore, the variables considered were limited to the 15 (+2) most demanded daily variables (see Table 1) selected from the list of 26 variables provided by C3S_34b Lot 1 for the European and Mediterranean domains (note that these two domains provide sub-daily information for some variables).

Number	Variable	Code	Units
1	Precipitation	pr	kg m ⁻² s ⁻¹
2	Mean surface air temperature	tas	K
3	Minimum surface air temperature	tasmin	K
4	Maximum surface air temperature	tasmax	K
5	Near-surface wind speed	sfcWind	m s ⁻¹
6	Near-surface specific humidity	huss	1
7	Near-surface wind speed (north-ward)	vas	m s ⁻¹
8	Near-surface wind speed (east-ward)	uas	m s ⁻¹
9	Near-surface relative humidity	hurs	%
10	Evaporation	evspsb1	kg m ⁻² s ⁻¹
11	Sea level pressure	psl	Pa
12	Surface Air Pressure	ps	Pa
13	Surface radiation (shortwave downwelling)	rsds	W m ⁻²
14	Surface radiation (longwave downwelling)	rlds	W m ⁻²
15	Total cloud fraction	clt	%
16	<i>Land area fraction (land/sea mask)</i>	sftlf	%
17	<i>Surface altitude</i>	orog	M

Table 1. List of surface climate variables (all at daily resolution) archived for the worldwide CORDEX dataset. Italics are used for spatial static variables (with no temporal axis), which provide information on the grid used by the models.

The worldwide CORDEX dataset provides data for the following experiments:

- **Evaluation (1980-2015, only 1990-2015 in some cases):** model simulations for the past with imposed "perfect" lateral boundary condition using ERA-Interim reanalysis.
- **Historical (1950-2005):** model simulations for the past using lateral boundary conditions from CMIP5 simulations under the historical scenario. These experiments are used as a reference for comparison with scenario runs for the future.
- **Scenario experiments RCP2.6, RCP4.5, RCP8.5 (2006-2100):** simulations driven by boundary conditions from CMIP5 scenario projections using RCP (Representative Concentration Pathways) forcing scenarios. The scenarios used are RCP 2.6, 4.5 and 8.5, as they provide different pathways of the future climate forcing.

The final ensemble for each domain was constructed considering all available simulations from all available resolutions (the standard 0.44° grid, and 0.11° and 0.22° grids when available), as listed in



the official CORDEX inventory³. The simulations were quality controlled (as described in D34d.1.3.1 and D34d.1.4.2) and some were discarded due to critical problems with the data (e.g. value ranges not consistent with the units, etc.). D34d.1.1.3 describes the final inventory for each domain and includes additional information for each simulation, such as the resolution, reasons for exclusion (if excluded), license, key references, etc.

Table 2 provides a summarized description of the number of simulations available domain by domain (in rows, see Figure 1 for the domain acronyms), indicating the number of RCMs and GCMs used in each domain, and the total number of available simulations for all scenarios (historical, RCP2.6, RCP4.5 and RCP8.5). The information is provided separately (in two blocks of columns) for the simulations which were available at ESGF (indicated by “ESGF”) and for the simulations gathered from local providers (indicated by “local”). More detailed information is available at D34d.1.1.3 (Table 3 thereof) which includes the individual details for the different resolutions and scenarios.

Domain	ESGF		Scenarios (RCPs)				local		Scenarios (RCPs)			
	RCM	GCMs	h	26	45	85	RCM	GCM	h	26	45	85
SAM	7	10	23	12	15	23	-	-	-	-	-	-
CAM	5	11	23	11	3	22	-	-	-	-	-	-
NAM	4	7	10	4	7	10	4	6	10	0	1	10
AFR	10	13	41	22	21	37	1	1	1	0	1	1
WAS	6	12	26	14	17	26	-	-	-	-	-	-
EAS	4	6	11	6	5	11	-	-	-	-	-	-
CAS	3	5	6	4	3	6	-	-	-	-	-	-
AUS	7	8	19	9	8	17	1	5	5	-	5	5
ANT	2	2	4	2	3	3	2	6	7	0	5	7
ARC	4	4	8	1	5	9	2	2	3	-	1	3
MNA	2	5	5	1	5	5	1	1	1	0	1	1
SEA	4	8	13	6	7	13	-	-	-	-	-	-

Table 2. Number of simulations available from ESGF and from local providers in the different CORDEX domains jointly for all resolutions. Historical and RCP 2.6, 4.5 and 8.5 scenarios are indicated by “h”, “26”, “45” and “85”, respectively.

The resulting information has been published under the C3S CDS catalogue “CORDEX regional climate model data on single levels”⁴ which includes a full description of the dataset, with the particular GCM-RCM combinations forming the ensembles for the different domains, as shown in Figure 2 for the case of the North America domain.

³ <https://cordex.org/data-access/regional-climate-change-simulations-for-cordex-domains>

⁴ <https://confluence.ecmwf.int/display/CKB/CORDEX%3A+Regional+climate+projections>

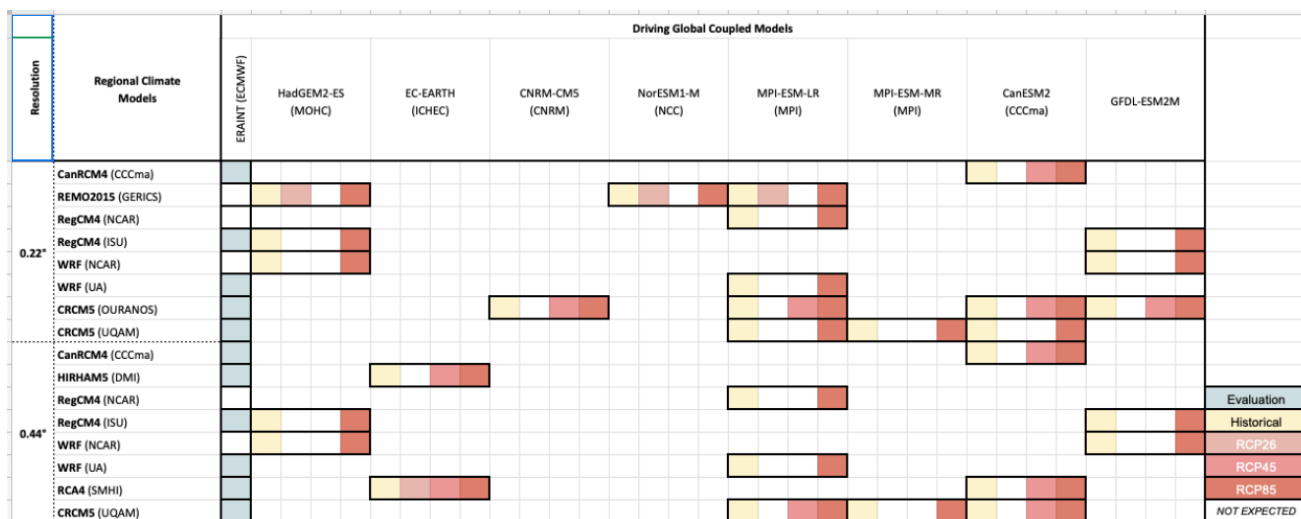


Figure 2. Schematic representation of the GCM/RCM combinations available for the illustrative North America domain, as included in the documentation of the C3S CDS catalogue “CORDEX regional climate model data on single levels”. Different colors indicate different scenarios.

The CORDEX dataset is distributed under the unrestricted version of the CORDEX terms of use⁵, with the exception of the simulations from the following RCMs: BOUN-RecCM4-3 model (for Central Asia and Middle East and North Africa) and RU-CORE-RegCM4-3 (for the South-East Asia domain), which are restricted to non-commercial use, according to the CORDEX terms of use.

2.1. The sub-ensemble CORDEX-CORE

CORDEX-CORE is an initiative under the umbrella of CORDEX designed to produce homogeneous regional projections for most of the inhabited land regions using nine of the CORDEX domains at 0.22° resolution (see Figure 1): North America (NAM), Central America (CAM), South America (SAM), Europe (EUR), Africa (AFR), South Asia (WAS), East Asia (EAS), Southeast Asia (SEA), and Australasia (AUS). Due to the computational requirements, three GCMs were selected to provide boundary conditions, covering the spread of high, medium, and low (HADGEM2ES, MPI-ESM, and NorESM, respectively) climate sensitivity from the CMIP5 ensemble at a global scale (using MIROC5, EC-Earth, GFDL-ES2M, respectively, as an alternative in case of regional problems with the former ones). CORDEX CORE focuses on two scenarios of low and high emission, RCP2.6 and RCP8.5, respectively. Two RCMs have contributed so far to this initiative (REMO and RegCM4) and a third one (COSMO-CLM) provides simulations over some of the domains.

This sub-ensemble of the worldwide CORDEX dataset constitutes a minimum homogeneous ensemble (six members) for climate change impact and adaptation studies, particularly those which require some data reduction approach due to computational constraints (e.g. running time-consuming impact models). CORDEX CORE simulations are distributed as part of the information available for the different CORDEX domains as listed in Table 2.

⁵ http://is-enes-data.github.io/cordex_terms_of_use.pdf



3. Description of the participant RCMs (model metadata)

The availability of comprehensive model documentation (metadata) is key to allow for an informed use of the data, considering key factors which may explain different model results (different parametrizations, use of dynamic aerosols, complexity of the land model, use of special components – lakes, cities, etc.). This is a time-consuming task and the CMIP community has developed technologies and tools to facilitate this, such as es-doc (<https://es-doc.org>). As a result, documentation of the contributing GCMs is available for the different CMIP versions (e.g. structured metadata is readily available for the CMIP5 global models used as boundary conditions for the CORDEX simulations⁶). Unfortunately, this is not the general case for the CORDEX initiative, which provides centralized and harmonized information on model documentation only for some models contributing to EURO-CORDEX⁷.

The activities of the C3S_34d contract have required close contact and exchange with the modeling centers contributing simulations for the different domains. This exchange of information has made it possible to update the existing inventories of simulations (see the previous section) and also to gather some common information on the different RCMs contributing to CORDEX regarding the atmosphere, aerosols, land, and ocean components (including key references and parameterizations used). This information constitutes the most comprehensive metadata available for the CORDEX ensemble and is a valuable resource for user guidance.

Table A1 in the appendix summarizes the information collected for the Regional Climate Models (RCMs) participating in the CORDEX experiment, with indication of the CORDEX domains they have contributed to, the institution producing the simulations, and details on the atmospheric, aerosols, land and ocean model components (including the precise parameterizations used, when available).

4. Assessment of regional overlaps

The multiple domains used in the worldwide CORDEX dataset overlap in different regions (e.g. the Mediterranean or Central Asia, see Figure 1) where users are confronted with multiple datasets (e.g. Euro- and Med-CORDEX for the Mediterranean) which could produce different messages. Here we present a first comprehensive worldwide analysis of the potential inconsistencies and conflicts arising in areas with overlapping domains, following the work by Legasa and co-authors⁸ that focused on the Mediterranean area. In order to avoid local gridbox variability and to summarize the results, we will use the new subcontinental climatic regions used in the IPCC Sixth Assessment Report (see Figure 3).

⁶ <https://search.es-doc.org/?project=cmip5&documentType=cim.1.software.ModelComponent>

⁷ <https://search.es-doc.org/?project=cordexp>

⁸ <https://doi.org/10.1029/2019GL086799>

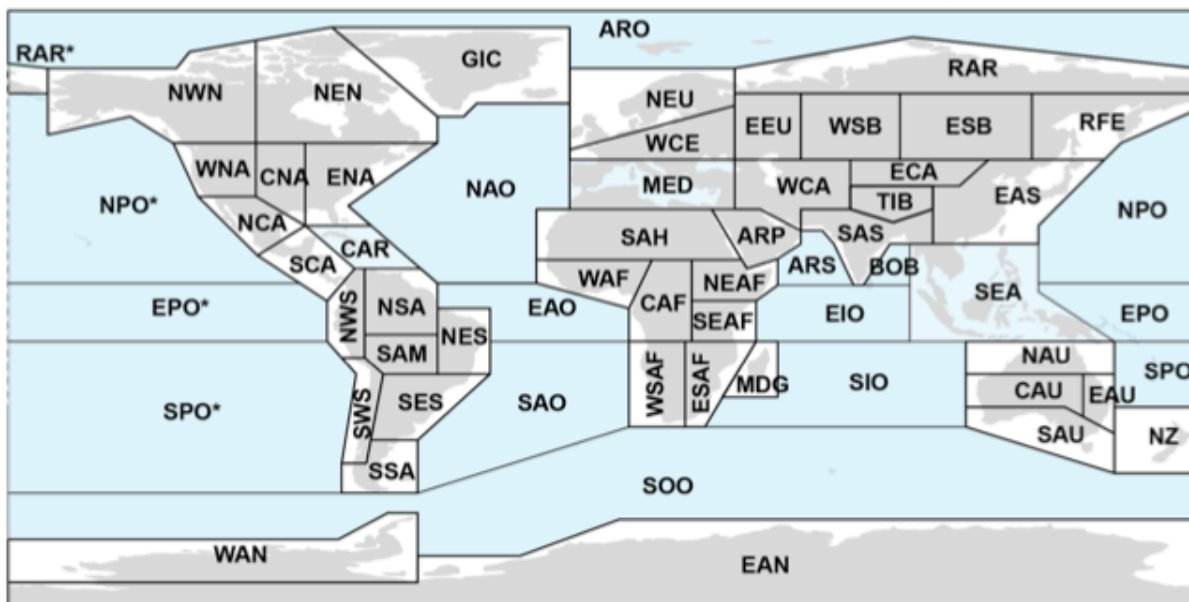


Figure 3. Updated IPCC reference regions showing 46 land (grey shading) and 15 ocean (blue shading) regions. IPCC AR6 WGI reference regions: **North America:** **NWN** (North-Western North America), **NEN** (North-Eastern North America), **WNA** (Western North America), **CNA** (Central North America), **ENA** (Eastern North America), **Central America:** **NCA** (Northern Central America), **SCA** (Southern Central America), **CAR** (Caribbean), **South America:** **NWS** (North-Western South America), **NSA** (Northern South America), **NES** (North-Eastern South America), **SAM** (South American Monsoon), **SWS** (South-Western South America), **SES** (South-Eastern South America), **SSA** (Southern South America), **Europe:** **GIC** (Greenland/Iceland), **NEU** (Northern Europe), **WCE** (Western and Central Europe), **EEU** (Eastern Europe), **MED** (Mediterranean), **Africa:** **MED** (Mediterranean), **SAH** (Sahara), **WAF** (Western Africa), **CAF** (Central Africa), **NEAF** (North Eastern Africa), **SEAF** (South Eastern Africa), **WSAF** (West Southern Africa), **ESAF** (East Southern Africa), **MDG** (Madagascar), **Asia:** **RAR** (Russian Arctic), **WSB** (West Siberia), **ESB** (East Siberia), **RFE** (Russian Far East), **WCA** (West Central Asia), **ECA** (East Central Asia), **TIB** (Tibetan Plateau), **EAS** (East Asia), **ARP** (Arabian Peninsula), **SAS** (South Asia), **SEA** (South East Asia), **Australasia:** **NAU** (Northern Australia), **CAU** (Central Australia), **EAU** (Eastern Australia), **SAU** (Southern Australia), **NZ** (New Zealand), **Small Islands:** **CAR** (Caribbean), **PAC** (Pacific Small Islands).

Two main approaches have been followed in the literature to produce worldwide homogeneous information merging the results provided by the different domains:

1. Mosaic of overlapped domains: The results from different domains are overlaid producing a mosaic, with a particular bottom-top order. This is the procedure typically followed in CORDEX-CORE, using a particular overlapping order: Central America, North America, South America, Europe, South East Asia, East Asia, South Asia, Australasia, Africa (the latter plotted on the top and hiding the preceding ones). In practice this means establishing a priority order of domains in the overlapping areas in terms which ones to be used. For instance, with the order above the Africa domain would have the highest priority and only model runs for the Africa domain would be used if there is an overlapping information from other domains.



2. Grand ensemble⁹: All available simulations across domains for each gridbox are pulled together. This approach maximizes the use of the information but generates a heterogeneous ensemble with varying ensemble size across regions. This may create spatial artifacts (e.g. border effects) in the results.

The mosaic approach avoids the potential artifacts which may arise in overlapping regions but may result in poor ensembles in regions with multiple information available from different domains. This approach allows using each domain for the area it was supposed to simulate best discarding boundary results. For instance, simulations from the South Asia domain might not represent properly the climatology of central Africa (if models are tuned to perform best in the South Asia region). However, most models don't tune the models for particular domains (with the exception of the Polar ones).

The preliminary analysis by Legasa and co-authors analyzed the uncertainty related to the choice of domain and showed that the variability of the climate change signal from the grand ensemble was mostly determined by the models, with little variability coming from the domain. Therefore, there is some evidence (in the Mediterranean) that the grand ensemble approach could be appropriate to enlarge the available ensembles of individual domains by pulling together the multi-domain simulations (avoiding duplicates of GCM-RCM pairs, or weighting them).

Here we extend this analysis analyzing all overlap regions in the worldwide CORDEX dataset. Figure 4 shows the number of simulations available from the worldwide CORDEX grand ensemble in each of the overlapping regions for the historical (top) and RCP2.6 (bottom) scenarios. This figure shows that the grand ensemble could be greatly beneficial in many regions (e.g. South Asia, Northern South America) allowing to enlarge the size of the ensemble.

Following the work by Legasa and coauthors, for a given overlapping reference region (e.g. Mediterranean), we intercompare the biases of the GCM-RCM pairs obtained from different domains. We follow the same procedure applied in D34d.3.3.1 to compute the model biases. Similar biases are an indication of a similar performance of the GCM-RCM pair, whereas different biases indicate differing behavior. Figures 5, 6, and 7 show the results for the relevant reference regions (those with larger overlaps) in Central and South America, Europe and Africa, and Asia, respectively. These figures show quite remarkable similarities between the model results obtained from different domains, with some particular differences. For instance, in general, the RCA model exhibit systematic warmer biases in the Central American domain (as compared to the South America one). For the SEAF region (and partially in NEAF), most regional models are warmer in the African domain than in the South Asia one.

These results extend the findings of the previous work by Legasa and coauthors and confirm that the grand ensemble approach could be appropriate to generate regional climate change information for specific applications, pulling together all available information.

⁹ First proposed in <https://doi.org/10.1175/JCLI-D-19-0084.1>

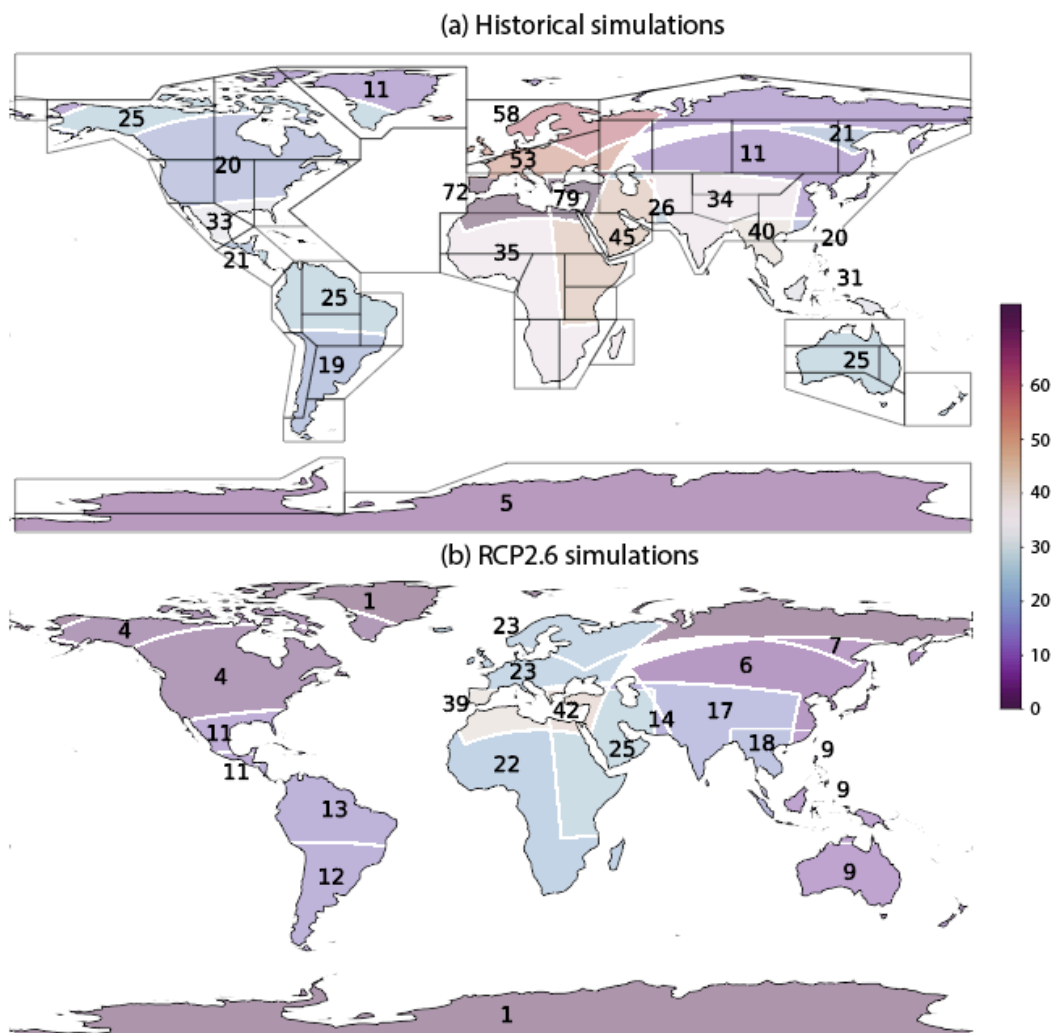


Figure 4. Number of simulations available from the worldwide CORDEX grand ensemble for the historical (top) and RCP2.6 (bottom) scenarios. Reference regions are overlaid on the top panel.

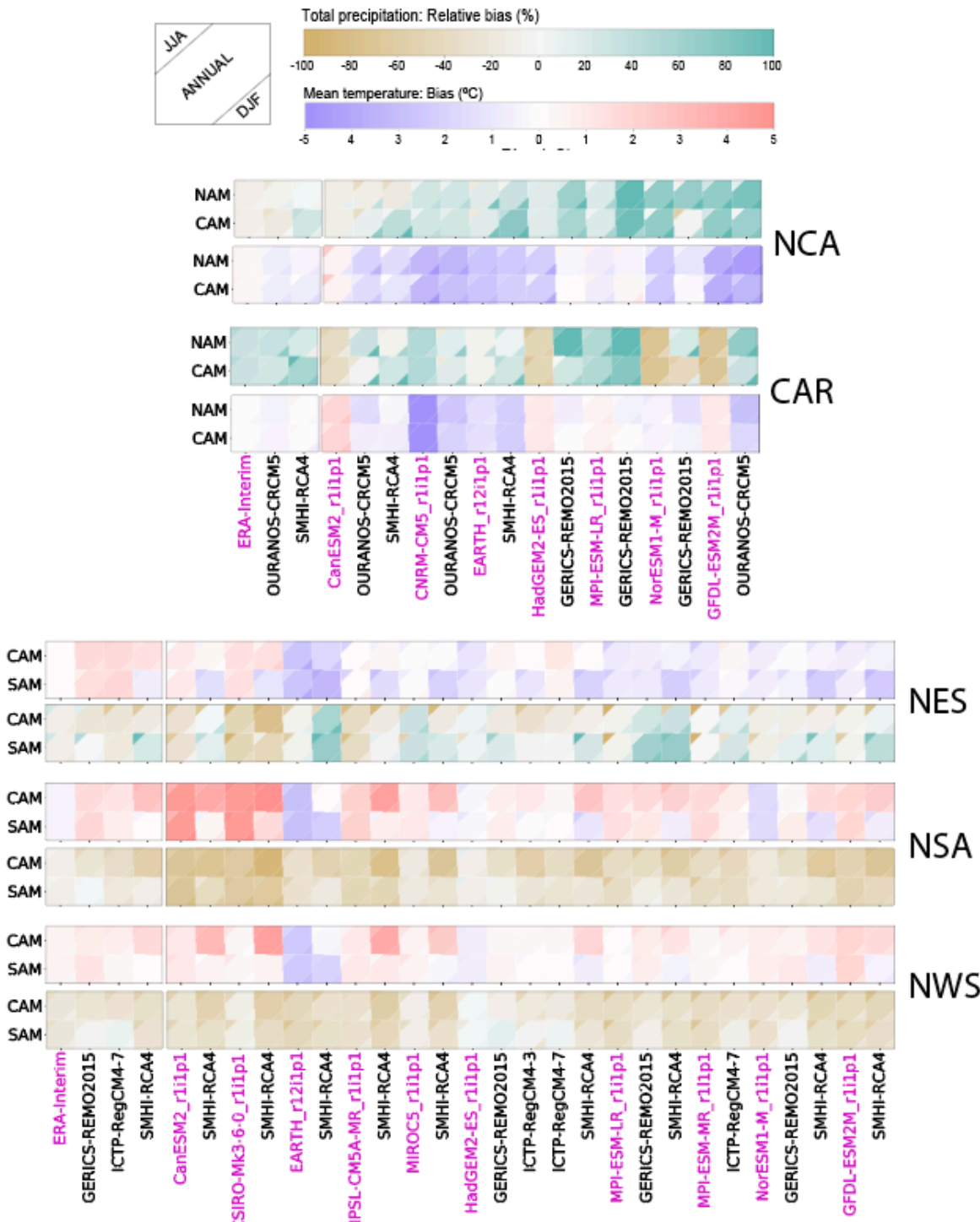


Figure 5. Biases of GCM-RCM pairs over the same geographical regions in Central and South America (right labels; see Figure 3) for precipitation and temperature resulting from different CORDEX domains (labels on the left; see Figure 1). GCM names are shown in magenta followed by the driven RCMs, which are shown in black.

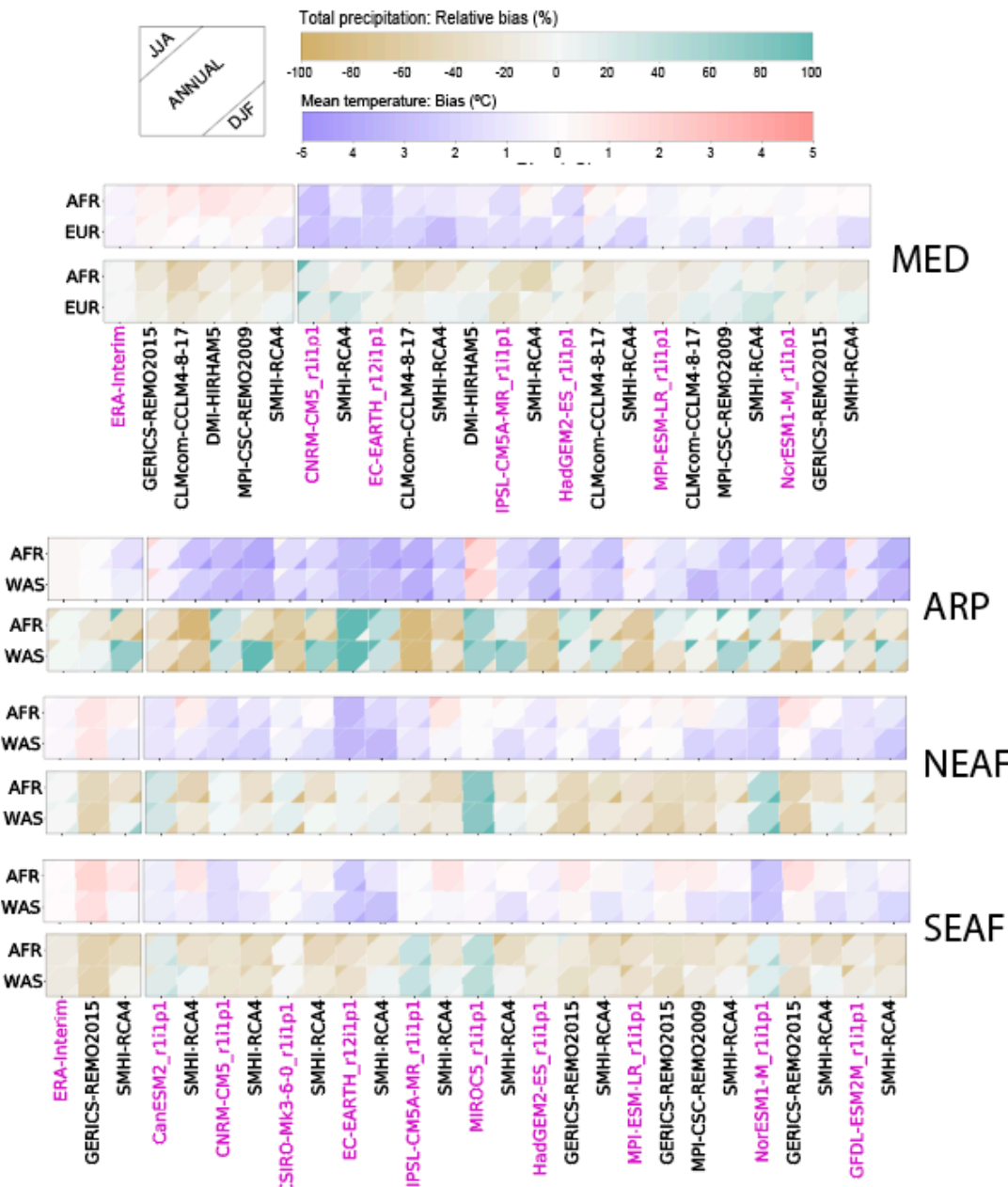


Figure 6. As Figure 5 but for regions in Europe and Africa.

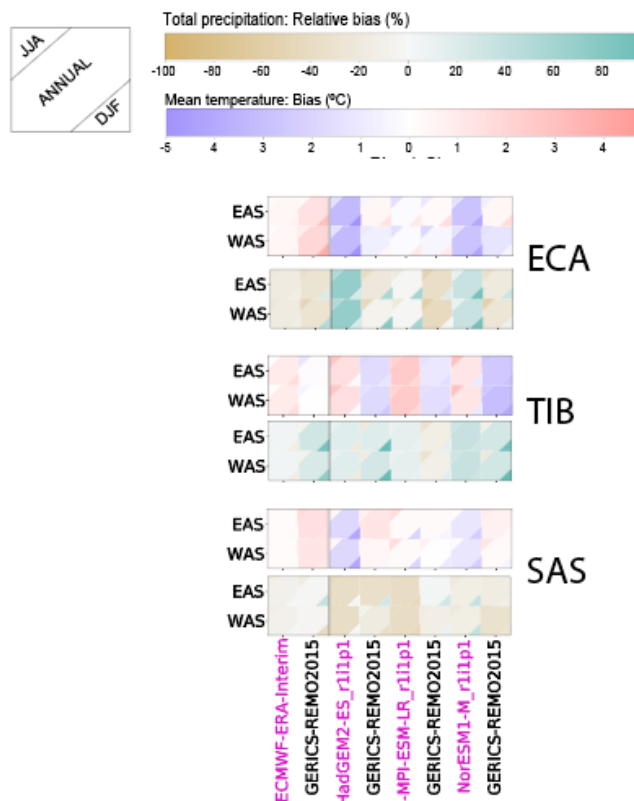


Figure 7. As Figure 5 but for regions in Asia.

5. Using the CDS Toolbox: Some common problems and solutions

The CDS Toolbox¹⁰ links raw data (such as the worldwide CORDEX dataset) to online computing power through a programming interface. It allows creating applications in Python and run them on the CDS computers, allowing to retrieve the data in, make the required calculations, and display the results. It a popular tool used among practitioners for data reduction and post-processing. In this section we provide some guidelines on the use of the Toolbox with the worldwide CORDEX dataset, presenting the common problems found due to the particularities of the dataset (rotated projections) and providing solutions. It is worth remarking that C3S is working on providing direct tools in the CDS catalogue entry to do subsetting, regridding and averaging. Therefore some of the following examples could be performed in the future directly from the CDS data access form.

Unlike other data in the CDS (like ERA5 or CMIP5), the CORDEX regional projections dataset is not available in a regular latitude-longitude grid. The data are indeed gridded, but they use different sets of coordinates (commonly called “projected” coordinates). The spherical (actually ellipsoidal) earth can be projected in a plane in many different ways. CORDEX data use different projections depending on the domain, to avoid excessive deformation. Sometimes the projection depends on the model too. For example, the ALADIN63 model over Europe uses a Lambert Conformal projection, while the

¹⁰ <https://cds.climate.copernicus.eu/toolbox/doc/index.html>



majority use a Rotated Latitude Longitude projection. These coordinate projections are the source of most of the problems when using CORDEX data. Here we explain the most common problems found and some recommendations to avoid them. As an example, we will use the data resulting for the following CDS Toolbox workflow, which access surface temperate data for a particular model (RACMO22E driven by EC-EARTH) for the historical year 1950.

```
import cdstoolbox as ct
@ct.application(title='Retrieve Data')
@ct.output.download()
def application():
    """
    Application main steps:

    - retrieve a variable from CDS Catalogue
    - produce a link to download it.
    """

    data = ct.catalogue.retrieve(
        'projections-cordex-domains-single-levels',
        {
            'domain': 'europe',
            'experiment': 'historical',
            'horizontal_resolution': '0_11_degree_x_0_11_degree',
            'temporal_resolution': 'monthly_mean',
            'variable': '2m_air_temperature',
            'gcm_model': 'icheck_ec_earth',
            'rcm_model': 'knmi_racmo22e',
            'ensemble_member': 'r1i1p1',
            'start_year': '1950',
            'end_year': '1950',
            'format': 'netcdf'
        },
    )
    # Average over time to reduce the size of the dataset in order to
    # speed up the tests
    data = ct.cube.average(data, dim="time")
    return data
```



5.1. Spatial subsetting

Selecting the data in a latitude longitude rectangular “box” is not as straightforward as with regular grids. This is because the region will not be rectangular in the projected coordinates. In the case of the CDS Toolbox, `cdstoolbox.cube.box_select` tool must be used.

```
data_box = ct.cube.box_select(data, lon=[-10., 5], lat=[35., 45.])
```

Do not use `cdstoolbox.cube.sel(data, lon=[-10., 5], lat=[35., 45.])`, as it will fail complaining that the lon, lat coordinates do not exist.

Without the toolbox, the user will find that lat and lon are 2D matrices in the NetCDF files. This expresses that the latitudes and the longitudes of each grid point depend on both the projected coordinates. In the case of the example we are following, the grid coordinates are Rotated Latitude and Longitude coordinates, called rlat and rlon:

```
<xarray.DataArray 'tas' (time: 12, rlat: 165, rlon: 155)>
dask.array<xarray-tas, shape=(12, 165, 155), dtype=float32,
chunksize=(12, 165, 155), chunktype=numpy.ndarray>
Coordinates:
  * rlon      (rlon) float32 -24.855 -24.745 -24.635 ... -8.135 -8.025 -
  7.915
    lon       (rlat, rlon) float64 dask.array<chunksize=(165, 155),
meta=np.ndarray>
  * rlat      (rlat) float32 -15.675 -15.565 -15.455 ... 2.145 2.255
  2.365
    lat       (rlat, rlon) float64 dask.array<chunksize=(165, 155),
meta=np.ndarray>
    height    float64 ...
  * time      (time) datetime64[ns] 1950-01-16T12:00:00 ... 1950-12-
  16T12:00:00
```

Functions such as `xarray.Dataset.where` must be used to filter the data in a box, passing them a boolean mask where the grid points inside the box we want to select are set to True and the rest to False. In order to make this mask we need to combine comparisons of the lat and lon arrays with the box boundaries. An efficient solution to do this in python is `numpy.logical_and` function:

```
mask = numpy.logical_and(
    numpy.logical_and(-10 <= lon, lon <= 5),
    numpy.logical_and(35 <= lat, lat <= 45)
)
data_box = dataset.where(mask)
```



5.2. Zonal and meridional averaging

In order to average these data over the latitudes or the longitudes, it is necessary to interpolate them to a regular latitude longitude grid. Interpolation tools are available in the CDS Toolbox (cdstoolbox.geo.regrid and cdstoolbox.geo.make_regular). For example:

```
data_box_regular = ct.geo.make_regular(data_box, xref="rlon",
yref="rlat")
# Then, to compute the zonal average, we would do
zonal_average = ct.cube.average(data, dim="lon")
```

If not using the Toolbox, the Climate Data Operators (cdo) or the xesmf python package are the recommended tools to carry on the regridding. Note that the interpolation method must be carefully chosen depending on the use case.

5.3. Model intercomparison and/or evaluation

In order to be able to compare the models between themselves or with gridded observations, they need to be in a common grid. If their grids differ, we will need to use an interpolation or regridding package. The common grid may be a regular latitude-longitude grid, or the one used by one of the models. Again, in the CDS toolbox, cdstoolbox.geo.regrid and cdstoolbox.geo.make_regular tools must be used. If not using the toolbox, the Climate Data Operators or the xesmf python package are the two suggested tools to be used.

5.4. Polar regions

Gridded data in polar regions can still be interpolated to a regular latitude longitude grid, but this will introduce a large deformation, and a singularity in the pole itself. The recommended way to use and to visualize these datasets are stereographical projections.

5.5. Plotting

cdstoolbox.map.plot does not currently work with projected data, so the data will need to be regridded to a regular grid before plotting it in the toolbox. Without the toolbox, the projected coordinates can be handled by the cartopy python package, although it can be difficult to get it to correctly plot some of the projections. The parameters supported by cartopy are described in <https://scitools.org.uk/cartopy/docs/latest/reference/generated/cartopy.crs.Projection.html>. The problem is that they are not always the same as the parameters defined in the CORDEX files metadata, and mapping between them can be difficult. To overcome this problem, cartopy can directly use the 2D lat lon matrices to plot the data in any projection. Also, regridding to a regular latitude grid, as usual, will remove most of these problems.



5.6. Common python workflow using CDSAPI, Xarray, Numpy, Cartopy, Matplotlib

A sample python script for retrieving data from the CDS (using the CDS API python client), computing a climatology (using Xarray and Numpy) and plotting a map (using Cartopy and Matplotlib):

```
import xarray as xr
import matplotlib.pyplot as plt
import cartopy.crs as ccrs
import cdsapi
import zipfile
import numpy

c = cdsapi.Client()
c.retrieve(
    'projections-cordex-domains-single-levels',
    {
        'domain': 'europe',
        'experiment': 'historical',
        'horizontal_resolution': '0_11_degree_x_0_11_degree',
        'temporal_resolution': 'monthly_mean',
        'variable': '2m_air_temperature',
        'gcm_model': 'icheck_ec_earth',
        'rcm_model': 'knmi_racmo22e',
        'ensemble_member': 'r1i1p1',
        'start_year': '1950',
        'end_year': '1950',
    },
    "download"
)

# CORDEX data is downloaded as zip file, so extraction is needed
with zipfile.ZipFile("download", "r") as zip_ref:
    names = zip_ref.namelist()
    zip_ref.extract(names[0])

# Loading data with Xarray and Netcdf
dataset_name = names[0]
data = xr.open_dataset(dataset_name)

# Performing spatial subsetting
mask = numpy.logical_and(
    numpy.logical_and(
        -10 <= data.lon, data.lon <= 5
    ),
    numpy.logical_and(
        35 <= data.lat, data.lat <= 45
    )
)
```



```
data_box = data.where(mask, drop=True)

# Perform temporal average
data_box_avg = data_box.mean(dim='time')

# Instance of plot with Xarray, Cartopy and Matplotlib:
plt.figure(figsize=(16, 9))
variable = 'tas'
# Select what to plot
to_plot = data_box_avg[variable]
# Select colormap palette
cmap = 'YlOrRd'
# Select the projection used and plot coastlines
ax = plt.axes(projection=ccrs.PlateCarree())
ax.coastlines() # temperature variable
contour = ax.contourf(to_plot.lon.values, to_plot.lat.values, to_plot,
cmap=cmap)
# Create a title describing some of the metadata attributes
attrs = data.attrs
title = f"tas variable for " \
\\
f"{ attrs['driving_model_id'] }_{ attrs['driving_model_ensemble_member'] }_" \
\\
f"{ attrs['institute_id'] }- \
{ attrs['model_id'] }_{ attrs['rcm_version_id'] }"
plt.title(title)
plt.colorbar(contour)
# Save the image
plt.savefig("download.png", bbox_inches='tight')
plt.clf()
plt.cla()
plt.close()
```

The resulting map:

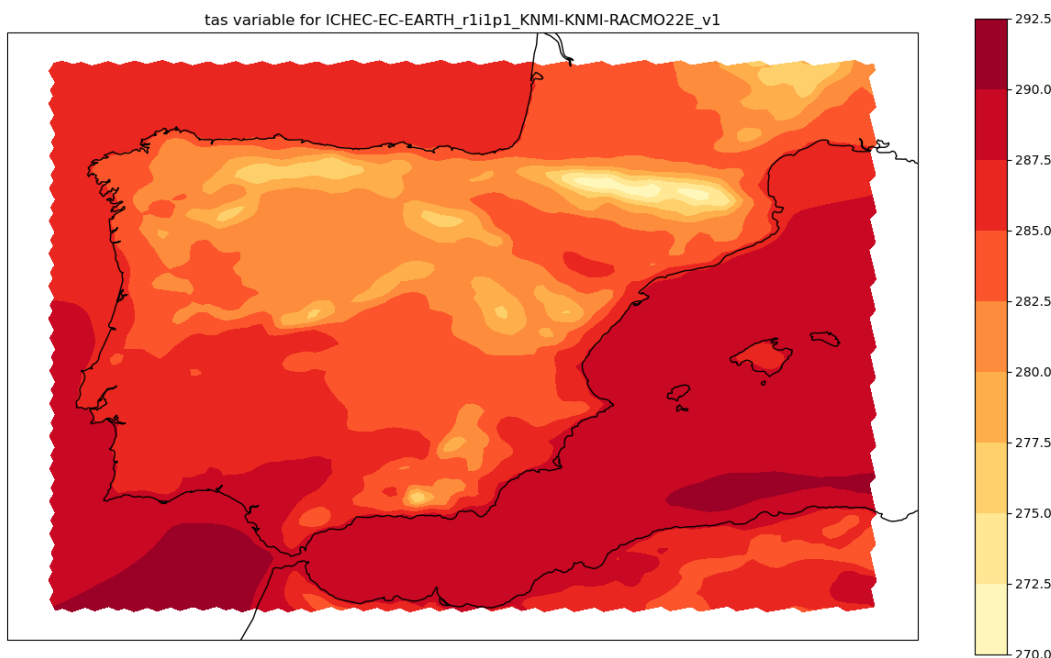


Figure 8. Plot of CORDEX data resulting from a python workflow using CDSAPI.

6. Conclusions

The C3S_34b Lot 1 & 2 (Europe and the Mediterranean) and C3S_34d (other regions) C3S contracts have produced a quality assured dataset of regional climate change projections gathering the simulations produced by the CORDEX community worldwide. The resulting dataset has been published at the CDS in the catalogue “CORDEX regional climate model data on single levels”. This has become an authoritative dataset for impact and adaptation studies and has been used in relevant international initiatives such as the IPCC AR6 (in particular in the Interactive Atlas¹¹).

This document describes the final dataset and provides some user guidance information. In particular, the Annex includes metadata documenting the models (different parametrizations, use of dynamic aerosols, complexity of the land model, use of special components – lakes, cities, etc.) that allows for an informed use of the dataset. Moreover, a preliminary analysis of the consistency of the dataset over overlapping regions is conducted reporting a large consistency of the results (with some small systematic differences). Finally, some guidelines on technical aspects are presented, illustrating how the CDS Toolbox can be used to work with this dataset, providing rather simple code to perform the most common tasks, and also discussing some common problems and solutions.

¹¹ <http://interactive-atlas.ipcc.ch>; <https://www.ipcc.ch/assessment-report/ar6/>



Annex. Metadata from the RCMs forming the dataset

Table A1. Metadata information of the Regional Climate Models (RCMs) participating in the CORDEX experiment, with indication of the domains where it is used, the institution producing the simulations, and details on the atmospheric, aerosols, land and ocean model components. Note that the information is missing for a few particular models.

Regional Climate Model (RCM)	Domains	Institutions [producing the runs] (city - for map)	Main references	Atmosphere	Aerosols	Land	Ocean	Additional components / comments
				1) number of levels 2) key parameterizations (or reference/link describing them; e.g. "described in main reference").	1) interactive or prescribed 2) component name (when interactive)	1) number of levels 2) component name	1) interactive or prescribed 2) component name 3) details	Lake, urban, or river models, etc. Comments on versions of the same model family.
ALADIN52_v1	['MED-44' 'MED-11' 'AFR-44']	['CNRM'] Toulouse	Colin et al. (2010) https://www.umr-cnrm.fr/spip.php?article125&lang=en	1) 31 2) CU: The convection scheme is a mass-flux scheme with convergence of humidity closure developed by Bougeault (1985) MP: Ricard and Royer (1993) statistical scheme and the large-scale precipitation is described by Smith (1990). PBL: Louis (1979) LW/SW: FMR based on Morcrette (1990) and from IFScy15. GHG (H2Ov, O3, CO2, CH4, N2O and CFC) Other: The orographic gravity wave scheme is based on Lott (1999). Interpolation of the wind speed from the first layer of the model (about 30 m) to the 10m height follows Geleyn (1988) .	1) prescribed (Szopa (2013) dataset) for eval and GCM forcing for scen runs, 5 classes, 2D spatial pattern, vertical profile, seasonal cycle, temporal evolution)	1) 3 2) ISBA (Noilhan J and Mahfouf J-F (1996))	Prescribed SST (ice cover defined by a SST threshold)	LK: no UR: no ALADIN53_v1 is same as ALADIN52_v1 except for the radiation scheme (RRTM for the LW, Mlawer et al. (1997) and FMR-6bands for the SW, Fouquart and Bonnel (1980); Morcrette et al. (2008), for the turbulent air-sea fluxes (ECUME) and for the mixing length based on Lenderink's work.
ALADIN53_v1	['EUR-11']							



ALADIN63_v1	['EUR-11']	['CNRM'] Toulouse	Nabat et al. (2020) https://www.umr-cnrm.fr/spip.php?article125&lang=en	1) 91 2) CU: PCMT; Piriou et al. (2007) and Guérémy (2011) MP: Lopez (2002) PBL: Cuxart et al. (2000) SW: Fouquart and Bonnel (1980), Morcrette et al. (2008) LW: based on RRTM (Mlawer et al., (1997)) Other: Air-sea turbulent fluxes are derived from the ECUME (Exchange Coefficients from Unified Multi-campaigns Estimates) iterative approach (Belamari and Pirani, 2007).	1) prescribed (TACTIC dataset for eval and GCM forcing for scen, 5 classes, 2D spatial pattern, vertical profile, seasonal cycle, temporal evolution)	1) 14 2) SURFEX8-ISBA (Decharme et al. (2019)). No land use land cover change is taken into account	Prescribed SST (ice cover defined by a SST threshold)	LK: Flake (Le Moigne et al. (2016)), prognostic lake ice. UR: Urban areas are considered as rock (Daniel et al. (2019)) ALADIN63_v1 and ALADIN63_v2 are identical. v2 label is used to indicate that the runs driven by the CNRM-CM5 GCM use the corrected version of the CNRM-CM5 Atmospheric-LBCs contrary to ALADIN53_v1
ALARO-0_v1	['EUR-11"CAS-22"]	['RMIB-UGent'] Brussels	Giot et al. (2016) Top et al. (2021)	1) 46 2) CU/MP/PBL: 3MT scheme (Gerard et al. 2009)	1) prescribed	1) 2 2) ISBA (Douville et al. 2000)	Prescribed SST	
CanRCM4_r2	['AFR-44' 'AFR-22' 'ARC-44' 'ARC-22' 'EUR-44' 'NAM-44' 'NAM-22']	['CCCma'] Victoria, B. C., Canada	Scinocca et al. (2016)	1) 25 2) described in main reference	1) interactive 2) "described in main reference"	1) 3 2) CLASS 2.7	Prescribed SST	Full atmospheric physics package identical to that used by parent global model, CanAM4, used by CanESM2 for CMIP5. Historical + RCP8.5 large ensemble (50 members) of 'NAM-44' available for large ensemble (50 members) of its parent model CanESM2.
CCAM_v1	['AFR-44i' 'ARC-44i' 'AUS-44i' 'CAM-44i' 'CAS-44i' 'EAS-44i' 'EUR-44i'	['CSIRO'] Melbourne	Hoffman et al. (2016)	1) 27 2) MP: Rotstayn (1997) and Lin et al. (1983) PBL: local-Ri closure McGregor et al (1993).	1) interactive 2) sulfate, black carbon, organic aerosol, mineral dust and sea salt Rotstayn and Lohman (2002) 8 and Rotstayn et al. (2011)	1) 6 2) CABLE (Kowalczyk et al. (2013))	Prescribed SST after bias and variance correction (CCAM_V1) or just bias correction (CCAM-1704_v1)). No atmospheric	UR: UCLEM (Lipson et al (2018))



	'MED-44' 'MNA-44' 'NAM-44' 'SAM-44' 'SEA-44' 'WAS-44' ['AUS-44i']			LW/SW: SEA-ESF (Freidenreich and Ramaswamy 1999, Schwarzkopf and Ramaswamy (1999)).			nudging.	
CCAM-1704_v1	['ANT-44i' 'AUS-44i']	['CSIRO'] Melbourne	Thatcher and McGregor (2009)	1) 35 2) MP: (Rotstainy (1983) and Lin et al (1983)) PBL: TKE closure Hurley (2007)) LW/SW: SEA-ESF (Freidenreich and Ramaswamy (1999), Schwarzkopf and Ramaswamy (1999)),	1) interactive 2) sulfate, black carbon, organic aerosol, mineral dust and sea salt Rotstainy and Lohman (2002) and Rotstainy et al (2011)	1) 6 2) CABLE (Kowalczyk, E et al (2013))	Prescribed SST	UR: UCLEM (Lipson et al 2018)
CCLM4-21-NEMOMFS_v1	['MED-44']	['CMCC'] Bologna						
CCLM4-8-17-CLM3-5_v1	['AUS-44']	['CLMcom'], city: Geesthacht	Virgilio er al. (2019)	1) 35 2) CU: Bechtold et al. (2008) MP: Seifert and Beheng (2001), reduced to one moment scheme. PBL: Prognostic TKE (Raschendorfer 2001) LW/SW: Ritter and Geleyn (1992).	1) Prescribed	1) 9 2) CLM (Dickinson et al. 2006)	Prescribed SST	
CCLM4-8-17_v1	['AFR-44' 'EUR-11']	['CLMcom']	Panitz et al. (2014),	1) 35 (AFR-44) 2) CU: Tiedtke (1989) MP: Seifert and Beheng (2001), reduced to one moment scheme PBL: Prognostic TKE closure (Raschendorfer 2001) LW/SW: Ritter and Geleyn (1992) Other: Subgrid-scale orography scheme: Lott and Miller (1997); Schulz (2008)	1) Prescribed	1) 9 2) soil-vegetation-atmosphere-transfer TERRA-ML (Schrodin and Heise, 2002).	Prescribed SST	
CCLM4-8-18_v1	['MED-44']	['GUF']						



CCLM4-8-19_v1	['MED-44']	['CMCC']						
CCLM4-8-19_v2	['MED-44']	['CMCC']						
CCLM5-0-15_v1	['AFR-22' 'AUS-22']	['CLMcom-HZG' 'CLMcom-KIT'] cities:Geest hacht for AUS-22, Karlsruhe for AFR-22		1) 57 2) CU: Bechtold et al. (2008) MP:Seifert and Beheng (2001), reduced to one moment scheme PBL: Prognostic TKE closure (Raschendorfer 2001) LW/SW: Ritter and Geleyn (1992) Other: Subgrid-scale orography scheme: Lott and Miller (1997), Schulz (2008).	1)Prescribed	1) 9 2) TERRA-ML (Schrodin and Heise, 2002).	Prescribed SST	LK: FLake (Mironov et al. 2010)
CCLM5-0-2_v1	['EAS-44']	['CLMcom']	Li et al. (2018)	1) 45 2) CU: Tiedtke (1989) MP:Seifert and Beheng (2001), LW/SW: Ritter and Geleyn (1992) Other: Subgrid-scale orography scheme: Lott and Miller (1997); Schulz (2008)	1)Prescribed: Aerosol optical thickness: NASA/GISS (Global Aerosol Climatology Project)	1) 9 Multilayer soil model TERRA-ML (Schrodin and Heise 2002)	Prescribed SST	Surface roughness: GLOBE (NOAA/NGDC); Global Land Cover 2000 Project (GLC2000)
CCLM5-0-9-NEMOMED12-3-6	['MED-11']	['CLMcom-GUF'] Frankfurt/Main https://wiki.coast.hzg.de/clmcom/cosmo-clm-98599047.html	Akhtar et al. (2018) https://wiki.coast.hzg.de/clmcom/cosmo-clm-98599047.html	1) 40 2) CU: Tiedtke (1989) MP: bulk microphysics parameterization including water vapour, cloud water, cloud ice, rain and snow LW/SW: Ritter and Geleyn (1992) PBL: Prognostic TKE closure Raschendorfer (2001).	1)Prescribed (a) AeroCom Global AOD data is used for Aerosol representation (Kinne S. et al. (2006))	1) 9 TERRA-ML (Schrodin and Heise, 2002).	1) Interactive 2) NEMOMED12 (1/12° resolution) is the interactive ocean model component (Beuvier et al. 2012). 3) The CCLM and NEMOMED12 models are coupled via OASIS3-MCT (Valcke 2013) with	RI: TRIP (Total Runoff Integrating Pathways) is used as the interactive river component for rivers over the Mediterranean Basin to feed runoff at the river mouths to the Mediterranean Sea (NEMOMED12)



							a 1-h coupling time.	
COSMO-crCLIM-v1-1_v1	['EUR-11' 'WAS-22']	['CLMcom-ETH'] Zürich	Leutwyler et al. 2017	1) 40 (EUR-11), 57 (WAS-22) 2) CU: adapted version of the Tiedtke (1989) MP: single-moment bulk scheme with 5 species (cloud water, cloud ice, rain, snow and graupel) PBL: Prognostic TKE closure Other parameterization schemes described in main reference Leutwyler et al. (2017) based on Baldauf et al. (2011): radiative transfer scheme, , multilayer soil model, and surface transfer scheme	1) prescribed: AeroCom1 aerosol monthly climatology dataset (Kinne et al., 2006).	1) 9 2) TERRA-ML with a soil hydrology scheme (Schlemmer et al. 2018)	Prescribed SST	COSMO-crCLIM is similar to CCLM. Its main characteristics are that it runs on GPUs and includes the soil hydrology scheme of Schlemmer et al (2018). Other adjustments include changing the upper level damping to only relax the vertical velocity instead of all dynamical fields (Klemp et al., 2008)
CRCM5_v1	['CAM-22' 'CAM-44' 'NAM-22']	['OURANOS'] Montreal, Canada	1)Martynov, A., et al, (2013). 2)Šeparović, L., et al. (2013).	1) 56 (TOA 10 hPa) 2) MP: modified Sandvik (1998); Bourguin (2000) ; CU: Kain andFritsch (1990), shCU: Kuo (1965) transient shallow, Non-cloudy boundary layer formulation. LW/SW: Li & Barker (2005) Other: vertical diffusion: Implicit vertical diffusion.	1) prescribed	1) 17 (to 15 m) 2) CLASS3.5c (Verseghy, 1993)	Prescribed SST SST & sea ice fraction	LK: Flake
CRCM5_v1	['AFR-22' 'AFR-44' 'ARC-22' 'ARC-44' 'NAM-11' 'NAM-22' 'NAM-44']	['UQAM'] Montreal	http://people.sca.uqam.ca/winger/CORDEX; Martynov, A. et al. (2013)	1) 56 (TOA 10 hPa) 2) CU: Kain and Fritsch (1990); MP: bourge3d; LW/SW: cccmarad	1) prescribed; Not varying in time; higher values at the equator, lower at the poles; higher values over land than over the ocean	1) 26 (to 60 m) 2) CLASS3.5+	1) prescribed SST & sea ice fraction	LK: FLake



				Other: vertical diffusion: clef; shallow convection: conres & ktrsnt;				
Eta_v1	['SAM-20']	['INPE'] Sao Paulo	Chou SC, et al. (2014a) Chou SC, et al. (2014b)	1) 38 (TOA 25hPa) 2) CU/shCU: Betts-Miller(1986) modified by Janjić (1994). MP: Zhao et al.(1997). PBL: Mellor-Yamada level 2.5; LW: Fels and Schwarzkopf (1975) SW: Lacis-Hansen (1974)	1) Prescribed	1) 4 2) NOAH scheme (Ek et al. 2003) 12 Vegetation types and 9 soil types.	1) Prescribed SST	No orography smoothing; No internal or lateral boundary relaxation nudging.
HIRHAM5_v1 HIRHAM5_v2 HIRHAM5_v3	['ANT-44' 'ARC-44' 'EAS-44' 'EUR-11' 'NAM-44'] [['AFR-44' 'EUR-11'] ['EUR-11']]	['DMI'] Copenhagen	O.B. Christensen et al. (2007).	1) 31 2) Same as GCM ECHAM5. See main reference.	1. Prescribed	1) 5 2) ECHAM5	1) Prescribed SST, Sea Ice	The different versions v1, v2, v3, are simulation versions due to necessary re-runs, not different model versions.
HadREM3-GA7-05_v1 HadREM3-GA7-05_v2	['EUR-11'] ['EUR-11']	['MOHC'] Exeter	Tucker et al. (2018) Dyn (submitted 2021) Walters et al. (2019)	1) 63 2) Walters et al. (2019) Other: no lake component, no stochastic physics	MACv2-SP dataset (Stevens et al, 2017), total aerosol properties, 9 bands EasyAerosol (Voigt et al. 2014) RCP scenarios	1) 4 2) Walters et al. (2019)	Prescribed SST and sea ice from driving GCM/reanalysis	LK: no The “v2” runs are using CNRM boundary conditions from pressure level 3d data. This is because CNRM model levels 3d data (the v1 version) do not correspond to the CNRM output available in the CMIP5 archive. No differences in the RCM, only a different source of lbc.
LMDZ4NEMOM_ED8_v1 LMDZ4NEMOM	['MED-44'] ['MED-44']	['LMD'] Paris, France	L'Heveder et al. (2013) Vadsaria et al.	1) 19 2) Li (1999), Hourdin et al. (2006).	1) prescribed	1) 2 2) ORCHIDEE	1) interactive 2) NEMOMED8 (Beuvier et al. (2010))	Rl: Interactive river coupling in v2. No river coupling in v1



ED8_v2		['LMD'] Paris, France	(2020)				32) Interactive Mediterranean Sea only, , 9-(120km with a tilted and stretched grid at the Gibraltar Strait, 43 vertical levels with a 6-m thick first level levelsL, daily coupling frequency by the OASIS coupler (Valcke (2013))	
MAR311_v1	['ANT-44']	['ULg' 'Ulg'] Liège (Belgique)	Agosta et al. (2019). Kittel et al. (2021).	1) 24 2) Hydrostatic (Gallée and Schayes, 1994). MP: Gallée (1995). LW/SW: Morcrette (2002)	Prescribed, RCP scenarios	1) 7 2) SISVAT (De Ridder and Schayes, 1997; De Ridder, (1997), (Gallée and Duynkerke, (1997); Gallée et al., (2001); Lefebre et al., (2003))	1) Prescribed SST and SIC (evolution of the snow properties simulated by SISVAT)	SISVAT model: 30 snow/ice layers over the ice sheet and two sub-pixels (rocs and permanent ice-covered area)
EBU-POM2c_v1	['MED-44i']	['UB'] Belgarde (Serbia)	Djurdjevic V. and Rajkovic B. (2008). Djurdjevic V. and Rajkovic B. (2010) Krzic A. et al. (2011)	1) 32 2) Hydrostatic, Eta vertical coordinate (Mesinger et al., 1988) CU: Bets-Miller-Janjic (Janjic, 1994) PBL: Mellor-Yamada-Janjic (Janjic, 2003) LW: Chou and Suarez (1994) SW: Chou (1992)	Prescribed	1) 4 2) NOAH-LSM (Ek et al. 2003)	POM - Princeton ocean model (30km, L21, coupling frequency 6 min)	
PROTHEUS_v2	['MED-44']	['ENEA'] C.R. Casaccia Roma	Artale V. et al. (2010). Soto-Navarro J. et al. (2020).	1) 18 2) CU: Grell (1993) with the Fritsch and Chappell (1980) closure assumption MP: Pal et al. (2000)	1) no active aerosol chemical model 2) n/a	1) 2 2) BATS1e Dickinson et al. (1993). Air-sea exchanges by Zeng et al. (1998) to	1) Interactive 2) MITMED8 (1/8° resolution) is the interactive ocean model component (Sannino G. et al.	RI: Fully interactive (daily coupling) using the TRIP river routine model



				LW/SW: CCM3 radiative transfer scheme (Kiehl et al.1996) with specified GHG concentrations PBL: Holtslag et al. (1990)		improve excessive evaporation from warm ocean surfaces (Pal et al.2007) in the original BATS package.	(2009))	
RACMO21P_v1 RACMO21P_v2	['ANT-44']	['KNMI'] De Bilt	vanMeijgaard et al. (2008)	1) 40 2) hydrostatic, with HIRLAM dynamical kernel (Undén et al. 2002) utilizing a 2-level semi-lagrangian advection scheme. Baseline physics is taken from the IFS CY23r4 ECMWF package of physical parameterizations. CU: EDMF-scheme; Siebesma et al., 2007	1) prescribed (Tegen et al., 1997) , four classes (land, maritime, dust, urban) + stratospheric + (optionally) volcanic	1) 4 2) baseline LSM TESSEL (van den Hurk et al.. 2000); Land-ice tile added for ice-sheet modelling. Multi-layer snow-ice-refreezing scheme (Ettema et al., (2010); snow albedo scheme (Munneke et al., 2011); snow drift scheme (Lenaerts et al., 2012)	1) prescribed SST and sea-ice concentration; inferred from from re-analysis or GCM	Model versions: Simulations with RACMO21P_v2 are straight reruns of RACMO21P_v1 employing the same model system and parameter settings. In ANT-44 simulations, v2 is only used with MOHC-HadGEM2-ES forcing to fix the remapping of SST to the RACMO grid in the v1-simulation
RACMO22E_v1 RACMO22E_v2	['EUR-11']	['KNMI'] De Bilt	van Meijgaard, et al. , (2012). http://climexp.knmi.nl/publications/FinalReport_KvR-CS06.pdf	1) 40 2) hydrostatic, with HIRLAM dynamical kernel (Undén et al. 2002) utilizing a 2-level semi-lagrangian advection scheme. Baseline physics is taken from the IFS CY31r1 ECMWF package of physical parameterizations. CU: EDMF-scheme; Siebesma et al., 2007; shCU: Neggers et al. 2009 MP: Neggers 2009; PBL: TKE Lenderink and Holtslag,	1)prescribed 2)inferred from CAM inventory (except volcanic); historical and rcp pathways (van Vuuren et al 2011; Lamarque et al. 2010; 2011); also used in evaluation Sulfate, particulate organic matter black carbon, sea salt, desert dust stratospheric aerosols, volcanic aerosol.	1) 4 2) HTESSEL (Balsamo et al. 2009)	1) prescribed SST and sea-ice concentration; inferred from from re-analysis or GCM	Model versions: Simulations with RACMO22E_v2 are straight reruns of RACMO22E_v1 employing the same model system and parameter settings. Meaning of v2 depends on forcing GCM: i) MOHC-HadGEM2-ES: remapping of GCM-SST to RACMO grid erroneous in v1, corrected in v2 ii) CNRM-CERFACS-CNRM-CM5: atmospheric forcings



				2004 Other: MODIS inferred leaf-area index.	Spatial maps and vertical profiles per species. Monthly variations and decadal trends.			derived from pressure level fields, because of error in CNRM-CM5 model level fields
RACMO22T_v1 RACMO22T_v2	['AFR-44']	['KNMI'] De Bilt	van Meijgaard, et al. , (2012). http://climexp.knmi.nl/publications/FinalReport_KvR-CS06.pdf	1) 40 2) hydrostatic, with HIRLAM dynamical kernel (Undén et al. 2002) utilizing a 2-level semi-lagrangian advection scheme. Baseline physics is taken from the IFS CY31r1 ECMWF package of physical parameterizations. CU: EDMF-scheme; Siebesma et al., 2007; shCU: Neggers et al. 2009 MP: Neggers 2009	1) prescribed 2) as in RACMO22E	1) 4 2) HTESSEL (Balsano et al. 2009)	1) prescribed SST and sea-ice concentration; inferred from from re-analysis of GCM	Model versions: Simulations with RACMO22T_v2 are straight reruns of RACMO22T_v1 employing the same model system and parameter settings. In AFR-44, v2 is only used with MOHC-HadGEM2-ES forcing to fix the remapping of SST to the RACMO grid in the v1-simulation
RCA4_v1 RCA4_v1a RCA4_v2 RCA4_v3 RCA4-SN_v1	['AFR-44' 'ARC-44' 'CAM-44' 'EUR-11' 'NAM-44' 'SEA-22'] ['EUR-11'] ['WAS-44'] ['SAM-44'] ['ARC-44']	['SMHI'] Norrköping	Strandberg et al. (2015). Samuelsson et al. (2015)	1) 40 2) CU: based on Bechtold- Kain-Fritsch (BKF) scheme (Bechtold et al. 2001) with revised calculation of CAPE profile according to Jiao and Jones (2008) MP: Rasch and Kristjansson (1998) PBL: TKE scheme (Lenderink & Holtslag 2004) LW/SW: Savijärvi (1990) and Sass et al. (1994) with the consideration of CO2 absorption and an improved treatment of the water vapour continuum (Räisänen et al. 2000)	1) "prescribed": single integrated class, parameterized aerosol effect on radiation fluxes, spatially uniform, static.	1) 3 2) a tile-based scheme with physiography based on ECOCLIMAP (Samuelsson et al. 2015)	1) Prescribed SST and sea(ice from driving GCMs/reanalysis 2) - 3) daily	LK: Flake (pronostic lake ice). Mironov et al. (2010) Model versions: i) RCA4-v1a is simply a re-run because a restart file to start the scenario experiment was taken from another simulations, ii) RCA4-v2 and RCA4-v3 are slightly tuned versions of RCA4-v1 (some parameters) but parameterizations are the same. RCA-SN indicates spectral nudging.
RCSM4_v1	['MED-44']	['CNRM'] Toulouse	Sevault et al. (2014) http://www.umr	1) 31 2) same as ALADIN52_v1	1) prescribed (Szopa et al. 2013 dataset for evaluation and GCM	1) 3 2) ISBA (Noilhan J, Mahfouf J-F	1) interactive 2) NEMOMED8 (Beuvier et al.	1) interactive rivers connecting the atmosphere to the ocean



			cnrm.fr/spip.php? article1098		forcing for scen runs, 5 classes, 2D spatial pattern, vertical profile, seasonal cycle, temporal evolution)	(1996))	(2010)) 3) Mediterranean Sea only, , 9-12km with a tilted and stretched grid at the Gibraltar Strait, 43 vertical levels with a 6-m thick first level , daily coupling frequency by the OASIS coupler (Valcke (2013))	2) TRIP (Oki and Sud 1998, Decharme et al., 2010) 3) 50km spatial resolution
REMO2009_v1	['AFR-44' 'EUR-11' 'SAM-44' 'WAS-44']	['GERICS' 'MPI-CSC'] Hamburg	Jacob and Podzun (1997)	1) 27 2) hydrostatic model built on Europa model dynamics and ECHAM physics. CU: Mass flux (Tiedtke, 1989) with modifications after Nordeng (1994) LW/SW: Morcrette et al. (1986) with modifications for additional greenhouse gases, 14.6 µm band of ozone and various types of aerosols. Continuum absorption after Giorgetta and Wild (1995).	1) prescribed (Tanré et al. 1984)	1) 5 2) a tile-based scheme including annual cycle of albedo (Rechid et al. 2009)	1) prescribed SST and SIC	REMO2009_v1 and REMO2015_v1 and V2 are essentially the same, just with some technical changes
REMO2015_v1	['AFR-22' 'AUS-22' 'CAM-22' 'CAS-22' 'EAS-22' 'EUR-11' 'NAM-22' 'SAM-22' 'SEA-22' 'WAS-22'] ['EUR-11']		Jacob (2001)					
REMO2015_v2								
ROM	['MED-22' 'SA-22' 'SEA-44' 'EUR-17'] ['MED-22' 'MED-44']	['GERICS' 'AWI']	Sein et al., (2015)	REMO model (see above)	See above	See above	Interactive. SST , SIC and SIT are calculated in ocean model MPIOM	1) interactive rivers connecting the atmosphere to the ocean 2) Hydrological Discharge (HD) model 3) 50km spatial
ROM_v1								
RRCM_v1	['ARC-44']	['MGO'] St Petersburg	Shkolnik and Efimov (2013)	1) 25 2) hydrostatic CU: Tiedtke (1989) LW/SW: Shneerov et al., 2001); PBL: Meleshko et al. (2014)	Prescribed	1) 4 2) MGO-2 (Shneerov et al., 2001)	Prescribed SST	



RegCM4-BATS_v1	['MED-44']	['ITU'] Istanbul	Ruti P. M. et al. (2016)	1) 18 2) CU: Grell MP: Explicit moisture (SUBEX; Pal et al 2000). PBL: Holtslag (1990) LW/SW: CCM radiation scheme (NCAR CCM3, Kiehl et al. 1998). RegESM 1) 23 2) CU: Emanuel (1991)	1) no active aerosol chemical model 2) n/a	1) 2 2) BATS1e	1) prescribed 2) no comp. 3) surface layer Zeng et al (1998) 1) ROMS-revision 809; Haidvogel et al., 2008)	In MED-11, Wave Model (WAM) Cycle-4 (4.5.3-MPI) coupled with Atmospheric model
RegESM	['MED-11']	['ITU'] Istanbul	Turuncoglu, U. U. (2019)					
RegCM4-3_v1	['MED-44']	['ELU' 'ICTP'] Budapest						
RegCM4-3_v4	['AFR-44' 'CAM-44' 'SAM-44' 'SEA-22' 'MED-11']	['ICTP' 'RU-CORE'] ICTP Trieste (SEA-22 RU-CORE Bangkok)	Giorgi et al. (2012)	1) 18 2) CU: [AFR-44] Emanuel (1991) over ocean, Grell over land; [CAM-44, SAM-44, SEA-22] Emanuel (1991) MP: Explicit moisture (SUBEX; Pal et al 2000). PBL: Holtslag (1990) LW/SW: CCM radiation scheme (NCAR CCM3, Kiehlet al, 1998). Other: LBC using Relaxation, exponential technique	1) no active aerosol chemical model 2) n/a	1) 2 2) BATS1e [SAM-44: 1) 10 2) CLM3.5]	1) prescribed 2) no comp. 3) surface layer Zeng et al (1998)	N/A
RegCM4-3_v5	['CAS-44' 'MNA-44']	['BOUN'] Istanbul	Ozturk et al. (2017) Ozturk et al. (2018)	1) 18 2) CU: Grell with Fritsch & Chappell (1980) closure. MP: Explicit moisture (SUBEX; Pal et al 2000). PBL: Holtslag (1990) LW/SW: CCM radiation scheme (NCAR CCM3, Kiehl et al. 1998). Other: LBC using Relaxation,	1) no active aerosol chemical model 2) n/a	1) 1 2) BATS 1e	1) prescribed 2) no comp. 3) surface layer Zeng et al (1998)	N/A



				exponential technique					
RegCM4-3_v7	['MED-44']	['EICTP']							
RegCM4-4_v0	['EAS-22']	['ICTP'] Trieste	Giorgi et al. (2012)	1) 18 2) CU: Emanuel (1991) MP: Explicit moisture (SUBEX; Pal et al 2000). PBL: Holtslag (1990) LW/SW: CCM radiation scheme (NCAR CCM3, Kiehl et al. 1998).	1) no active aerosol chemical model 2) n/a	1) 2 2) BATS1e	1) prescribed 2) no comp. 3) surface layer Zeng et al (1998)	N/A	
RegCM4-4_v5	['WAS-44']	['IITM'] Pune	Giorgi et al. (2012), Sanjay et al. (2017), Sanjay et al. (2020)	1) 18 2) CU: Emanuel (1991) MP: Explicit moisture (SUBEX; Pal et al 2000). PBL: UW (Bretherton et al , 2004) LW/SW: CCM radiation scheme (NCAR CCM3, Kiehl et al., 1996).	1) no active aerosol chemical model 2) n/a	1) 10 2) CLM4.5	1) prescribed 2) no comp. 3) surface layer Zeng et al (1998)	UR: CLM4.5	
RegCM4-6_v1	['EUR-11']	['ICTP'] Trieste	Giorgi et al. (2012)	1) 23 2) CU: Tiedtke (1996) MP: Explicit moisture (SUBEX; Pal et al 2000). PBL: UW (Bretherton and McCaa, 2004) LW/SW: CCM radiation scheme (NCAR CCM3, Kiehl, 1998).	1) no active aerosol chemical model 2) n/a	1) 10 2) CLM4.5	1) prescribed 2) no comp. 3) surface layer Zeng et al (1998)	UR: CLM4.5	
RegCM4-7_v0	['AFR-22' 'AUS-22' 'CAM-22' 'SAM-22' 'SEA-22' 'WAS-22']	['ICTP' 'ORNL'] Trieste, Italy and Oak ridge, TN, USA	Giorgi et al. (2012)	1) 23 2) CU:[AFR-22, SAM-22] Tiedtke (1996) land, Kain and Fritsch (1990), Kain (2004) over ocean; [AUS-22, SEA-22] Tiedtke (1996); [CAM-22] Emanuel (1991) over land, Kain and Fritsch (1990), Kain (2004) over ocean. [WAS-22]	1) no active aerosol chemical model 2) n/a	1) 10 2) CLM4.5	1) prescribed 2) no comp. 3) surface layer Zeng et al (1998)	UR: CLM4.5	



				Emanuel (1991) over land, Tiedtke (1996) over ocean. MP: Explicit moisture (SUBEX; Pal et al 2000). PBL: Holtslag (1990) LW/SW: CCM radiation scheme (NCAR CCM3, Kiehl et al., 1998).				
RegCM4_v4-4-rc8	['NAM-22']	['ISU' 'NCAR'] Ames, IA, USA and Boulder, CO, USA	Giorgi et al., (2012) Bukovsky and Mearns (2020), Mearns et al. (2017)	1) 18 2) https://na-cordex.org/rcm-characteristics.html (https://doi.org/10.5065/D6SJ1JCH) CU: Grell with Fritsch-Chappell closure over land; Emanuel (1991) over water MP: SuBEX PBL: Holtslag (1990) LW/SW: Kiehl		1) 3 soil layers 2) BATS	1) prescribed 3) SST prescribed; no sea-ice, prescribed atmospheric skin temperature instead	LK: Hostetler et al. 1993
EBU	['MED-44i']	['UB'] Belgarde (Serbia)	Same as EBU-POM2c_v1	1) Same as EBU-POM2c_v1	Same as EBU-POM2c_v1	Same as EBU-POM2c_v1	Prescribed SST	
WRF3.1.1_v1	['MED-11']	['IPSL']						
WRF341I_v2	['EUR-44', 'SAM-44']	['UCAN'] Santander, Spain	Skamarock et al. (2008)	1) 30 2) Advanced Research WRF (ARW) dynamical core (Skamarock et al 2008.) CU: Kain-Fritsch (Kain, 2004) MP: WRF single moment 5 class (WSM5, Hong et al., 2004)) PBL: YSU (Hong et al.,2006) LW/SW: CAM/CAM (Collins et al., 2004)	1) Prescribed uniform background with vertical profile. Constant in time.	1) 4 2) Noah (Chen and Dudhia, 2001)	1) Prescribed SST and sea-ice	WRF v3.4.1. "I" stands for the coordinated physics configuration used within CORDEX. "v2" refers to the variable GHG input and noleap calendar in scenario (CanESM2) simulations. Otherwise, fully comparable to v1 in ERA-Interim (fixed GHG, standard cal.)
WRF351_v1	['MNA-44']	['CYI'], Nicosia, Cyprus	Zittis et al. (2014), Zittis and Hadjinicolaou (2017)	1) 30 2) Advanced Research WRF (ARW) dynamics (Skamarock et al 2008) CU: Kain-Fritsch (Kain, 2004) MP: WSM6 (Hong & Lim, 2006) PBL: YSU (Hong et al.,2006)	1) Prescribed	1) 4 2) Noah (Chen and Dudhia, 2001)	Prescribed SST	



				LW/SW: CAM (Collins et al., 2004)				
WRF360J_v1	['AUS-44']	['UNSW'] Sydney	Powers et al. (2017), Evans et al. (2020)	1) 30 2) Advanced Research WRF (ARW) dynamics (Skamarock et al 2008) CU: Kain-Fritsch (Kain, 2004) MP: WRF double moment 5 class (WDM5; Lim and Hong, 2010) PBL: Mellor-Yamada-Janjic (Janjic, 1994) LW: RRTM (Mlawer et al., 1997) SW: Dudhia (1989)	1) Prescribed	1) 4 2) Noah (Chen and Dudhia, 2001)	Prescribed SST (ice with SST threshold)	
WRF360K_v1	['AUS-44']	['UNSW'] Sydney	Powers et al. (2017); Evans et al. (2020)	1) 30 2) Advanced Research WRF (ARW) dynamics (Skamarock et al 2008) CU: Betts-Miller-Janjic (Janjic, 1994) MP: WRF double moment 5 class (WDM5; Lim and Hong, 2010) PBL: Mellor-Yamada-Janjic (Janjic, 1994) LW: RRTM (Mlawer et al., 1997) SW: Dudhia (1989)	1) Prescribed	1) 4 2) Noah (Chen and Dudhia, 2001)	Prescribed SST (ice with SST threshold)	
WRF360L_v1	['AUS-44']	['UNSW'] Sydney	Powers et al. (2017); di Virgilio et al. (2019)	1) 30 2) Advanced Research WRF (ARW) dynamics (Skamarock et al 2008) CU: Kain-Fritsch (Kain, 2004) MP: WRF double moment 5 class (WDM5; Lim and Hong, 2010) PBL: YSU (Hong et al., 2006) LW/SW: CAM/CAM (Collins et al., 2004)	1) Prescribed	1) 4 2) Noah (Chen and Dudhia, 2001)	Prescribed SST (ice with SST threshold)	
WRF361H_v1	['EUR-11']	['UHOH <td>Skamarock, W. C. et al. (2008).</td> <td>1) 50 2) Advanced Research WRF dynamics (Skamarock et al 2008.) CU: Kain-Fritsch-Eta (Kain, 2004) MP: Morrison two-moment (Morrison et al., 2009) PBL: YSU (Hong et al., 2006) LW/SW: CAM/CAM (Collins et al.,</td> <td>1) Prescribed uniform background with vertical profile. Constant in time.</td> <td>1) 4 2) NOAH (Chen and Dudhia, 2001)</td> <td>Prescribed SST (ice with SST threshold)</td> <td></td>	Skamarock, W. C. et al. (2008).	1) 50 2) Advanced Research WRF dynamics (Skamarock et al 2008.) CU: Kain-Fritsch-Eta (Kain, 2004) MP: Morrison two-moment (Morrison et al., 2009) PBL: YSU (Hong et al., 2006) LW/SW: CAM/CAM (Collins et al.,	1) Prescribed uniform background with vertical profile. Constant in time.	1) 4 2) NOAH (Chen and Dudhia, 2001)	Prescribed SST (ice with SST threshold)	



				2004).				
WRF381_v1	['EUR-44'MED-44']	['CRC'] Dijon	https://doi.org/10.25666/dataosu-2021-03-05-02 https://doi.org/10.25666/dataosu-2021-03-05	1) 50 2) Advanced Research WRF dynamics (Skamarock et al 2008.) CU: Kain-Fritsch (Kain, 2004) MP: Morrison 2-moment (Morrison et al., 2009) PBL: YSU (Hong et al., 2006) LW/SW: RRTMG/RRTMG (Iacono et al., 2008)	1) Prescribed Tegen et al. (1997)	1) 4 2) Noah_mp (Niu et al. 2011) Modis land categories	Prescribed SST (ice with SST threshold) from global model	Allow sub-grid cloud fraction interaction with radiation (Alapaty et al. 2012) The forcing variables have been bias-corrected using ERA-Interim fields for 1981-2005, as in Bruyere et al. (2014).
WRF381P_v1	['EUR-11']	['IPSL'] Paris	Skamarock et al (2008)	1) 31 2) CU: New Arakawa-Schubert with deep and shallow convection (Han and Pan 2011) MP: New Thompson scheme (Thompson et al 2008) LW/SW: RRTMG/RRTMG (Iacono et al 2008) PBL: MYNN (Nakanishi & Niino, 2004)	Prescribe aerosols	1) 4	Prescribed SST and sea ice (from global model)	
WRF381P_v2	['EUR-11']	['IPSL'] Paris	Skamarock et al (2008)	same as WRF381P_v1	Same as WRF381P_v1	Same as WRF381P_v1	Same as WRF381P_v1	
WRF_v3-5-1	['NAM-22']	['NCAR' 'UA'] Boulder, CO, USA and Tucson, AZ, USA	Skamarock et al (2008). Mearns et al. (2017). Bukovsky and Mearns (2020).	1) 28 2) https://na-cordex.org/rcm-characteristics.html (https://doi.org/10.5065/D6SJ1JCH) CU: Kain-Fritsch (Kain, 2004) MP: WSM3 (Hong & Lim, 2006) PBL: MYJ (Janjic, 1994) LW: RRTM (Mlawer et al., 1997) SW: Goddard (Chou & Suarez, 1999)	1) Prescribed	1) 4 soil levels 2) Noah	Prescribed SST, prescribed sea-ice for GFDL and MPI-driven simulations, sea-ice with an SST threshold for HadGEM-driven simulation	WRF v3.5.1 Spectral nudging used.



References from Table A.1

- A. Voigt, O. B., B. Stevens, S. Bony. (2013). *The HIRHAM Regional Climate Model. Version 5 (beta)*. Danish Climate Centre, Danish Meteorological Institute. Denmark. Danish Meteorological Institute. Technical Report No. 06-17 <http://www.dmi.dk/dmi/tr06-17>.
- Agosta, C., Amory, C., Kittel, C., Orsi, A., Favier, V., Gallée, H., Broeke, M. R. van den, Lenaerts, J. T. M., Wessem, J. M. van, Berg, W. J. van de, & Fettweis, X. (2019). Estimation of the Antarctic surface mass balance using the regional climate model MAR (1979–2015) and identification of dominant processes. *The Cryosphere*, 13(1), 281–296. <https://doi.org/10.5194/tc-13-281-2019>
- Akhtar, N., Brauch, J., & Ahrens, B. (2017). Climate modeling over the Mediterranean Sea: Impact of resolution and ocean coupling. *Clim Dyn*, 51(3), 933–948. <https://doi.org/10.1007/s00382-017-3570-8>
- Alapaty, K., Mathur, R., Pleim, J., Hogrefe, C., Rao, S. T., Ramaswamy, V., Galmarini, S., Schaap, M., Makar, P., Vautard, R., Baklanov, A., Kallos, G., Vogel, B., & Sokhi, R. (2012). New Directions: Understanding interactions of air quality and climate change at regional scales. *Atmospheric Environment*, 49, 419–421. <https://doi.org/10.1016/j.atmosenv.2011.12.016>
- Artale, V., Calmanti, S., Carillo, A., Dell'Aquila, A., Herrmann, M., Pisacane, G., Ruti, P. M., Sannino, G., Struglia, M. V., Giorgi, F., Bi, X., Pal, J. S., & Rauscher, S. (2009). An atmosphere–ocean regional climate model for the Mediterranean area: Assessment of a present climate simulation. *Clim Dyn*, 35(5), 721–740. <https://doi.org/10.1007/s00382-009-0691-8>
- Baldauf, M., Seifert, A., Förstner, J., Majewski, D., Raschendorfer, M., & Reinhardt, T. (2011). Operational Convective-Scale Numerical Weather Prediction with the COSMO Model: Description and Sensitivities. *Monthly Weather Review*, 139(12), 3887–3905. <https://doi.org/10.1175/mwr-d-10-05013.1>
- Balsamo, G., Viterbo, P., Beijars, A., van den Hurk, B., Hirschi, M., Betts, A. K., & Scipal, K. (2009). A revised hydrology for the ECMWF model: Verification from field site to terrestrial water storage and impact in the integrated forecast system. *Journal of Hydrometeorology*, 10(3), 623–643. <https://doi.org/10.1175/2008JHM1068.1>
- Balsamo, Gianpaolo, Beljaars, A., Scipal, K., Viterbo, P., Hurk, B. van den, Hirschi, M., & Betts, A. K. (2009). A Revised Hydrology for the ECMWF Model: Verification from Field Site to Terrestrial Water Storage and Impact in the Integrated Forecast System. *Journal of Hydrometeorology*, 10(3), 623–643. <https://doi.org/10.1175/2008jhm1068.1>
- Bechtold, P., Bazile, E., Guichard, F., Mascart, P., & Richard, E. (2001). A mass-flux convection scheme for regional and global models. *Q.J. Royal Met. Soc.*, 127(573), 869–886. <https://doi.org/10.1002/qj.49712757309>
- Bechtold, Peter, Köhler, M., Jung, T., Doblas-Reyes, F., Leutbecher, M., Rodwell, M. J., Vitart, F., & Balsamo, G. (2008). Advances in simulating atmospheric variability with the ECMWF model: From synoptic to decadal time-scales. *Quarterly Journal of the Royal Meteorological Society*, 134(634), 1337–1351. <https://doi.org/10.1002/qj.289>



Belamari, S., & Pirani, A. (2007). *Validation of the optimal heat and momentum fluxes using the ORCA2-LIM global ocean-ice model, Marine Environment and Security for the European Area – Integrated Project (MERSEA IP), Deliverable D4.1.3, 88 pp.*

Bent Hansen Sass, P. R., Laura Rontu. (1994). *HIRLAM-2 Radiation Scheme: Documentation and Tests. HIRLAM technical report no 16, Norrköping, SWEDEN.* http://hirlam.org/index.php/hirlam-documentation/doc_view/1307-hirlam-technical-report-no-16.

Betts, A. K., & Miller, M. J. (1986). A new convective adjustment scheme. Part II: Single column tests using GATE wave, BOMEX, ATEX and arctic air-mass data sets. *Q.J Royal Met. Soc.*, 112(473), 693–709. <https://doi.org/10.1002/qj.49711247308>

Beuvier, J., Sevault, F., Herrmann, M., Kontoyiannis, H., Ludwig, W., Rixen, M., Stanev, E., Béranger, K., & Somot, S. (2010). Modeling the Mediterranean Sea interannual variability during 1961–2000: Focus on the Eastern Mediterranean Transient. *J. Geophys. Res.*, 115(C8). <https://doi.org/10.1029/2009jc005950>

Bøssing Christensen, A., O. , Drews, M. , Hesselbjerg Christensen, J. , Dethloff, K. , Ketelsen, K. , Hebestadt, I. , & Rinke. (2007). *The HIRHAM Regional Climate Model. Version 5 (beta). Danish Climate Centre, Danish Meteorological Institute. Denmark. Danish Meteorological Institute. Technical Report No. 06-17*<http://www.dmi.dk/dmi/tr06-17>.

Bougeault, P. (1985). A Simple Parameterization of the Large-Scale Effects of Cumulus Convection. *Mon. Wea. Rev.*, 113(12), 2108–2121. [https://doi.org/10.1175/1520-0493\(1985\)113<2108:aspotl>2.0.co;2](https://doi.org/10.1175/1520-0493(1985)113<2108:aspotl>2.0.co;2)

Bourguin, P. (2000). A Method to Determine Precipitation Types. *Wea. Forecasting*, 15(5), 583–592. [https://doi.org/10.1175/1520-0434\(2000\)015<0583:amtdpt>2.0.co;2](https://doi.org/10.1175/1520-0434(2000)015<0583:amtdpt>2.0.co;2)

Bretherton, C. S., McCaa, J. R., & Grenier, H. (2004). A New Parameterization for Shallow Cumulus Convection and Its Application to Marine Subtropical Cloud-Topped Boundary Layers. Part I: Description and 1D Results. *Mon. Wea. Rev.*, 132(4), 864–882. [https://doi.org/10.1175/1520-0493\(2004\)132<0864:anpfsc>2.0.co;2](https://doi.org/10.1175/1520-0493(2004)132<0864:anpfsc>2.0.co;2)

Bruyère, Cindy L., Done, J. M., Holland, G. J., & Fredrick, S. (2013). Bias corrections of global models for regional climate simulations of high-impact weather. *Clim Dyn*, 43(7–8), 1847–1856. <https://doi.org/10.1007/s00382-013-2011-6>

Bruyère, C.L., Done, J. M., Holland, G. J., & Fredrick, S. (2014). Bias corrections of global models for regional climate simulations of high-impact weather. *Climate Dynamics*, 43(7–8), 1847–1856. <https://doi.org/10.1007/s00382-013-2011-6>

Bukovsky, M. S., & Mearns, L. O. (2020). Regional climate change projections from NA-CORDEX and their relation to climate sensitivity. *Climatic Change*, 162(2), 645–665. <https://doi.org/10.1007/s10584-020-02835-x>

Chen, F., & Dudhia, J. (2001). Coupling an Advanced Land Surface–Hydrology Model with the Penn State–NCAR MM5 Modeling System. Part I: Model Implementation and Sensitivity. *Mon. Wea. Rev.*, 129(4), 569–585. [https://doi.org/10.1175/1520-0493\(2001\)129<0569:caalsh>2.0.co;2](https://doi.org/10.1175/1520-0493(2001)129<0569:caalsh>2.0.co;2)



Chou, M.-D., & Suarez, M. J. (1994). *An Efficient Thermal Infrared Radiation Parameterization for Use in General Circulation Models*. NASA Technical Memorandum No. 104606, Vol. 3, 85 p. Https://archive.org/details/nasa_techdoc_19950009331.

Chou, M.-D., & Suarez, M. J. (1999). *A Solar Radiation Parameterization (CLIRAD-SW) Developed at Goddard Climate and Radiation Branch for Atmospheric Studies*. NASA Technical Memorandum NASA/TM-1999-104606.

Chou, Ming-Dah. (1992). A Solar Radiation Model for Use in Climate Studies. *J. Atmos. Sci.*, 49(9), 762–772. [https://doi.org/10.1175/1520-0469\(1992\)049<0762:asrmfu>2.0.co;2](https://doi.org/10.1175/1520-0469(1992)049<0762:asrmfu>2.0.co;2)

Chou, S. C., Lyra, A., Mourão, C., Dereczynski, C., Pilotto, I., Gomes, J., Bustamante, J., Tavares, P., Silva, A., Rodrigues, D., Campos, D., Chagas, D., Sueiro, G., Siqueira, G., Nobre, P., & Marengo, J. (2014). Evaluation of the Eta Simulations Nested in Three Global Climate Models. *AJCC*, 03(05), 438–454. <https://doi.org/10.4236/ajcc.2014.35039>

Colin, J., Déqué, M., Radu, R., & Somot, S. (2010). Sensitivity study of heavy precipitation in Limited Area Model climate simulations: Influence of the size of the domain and the use of the spectral nudging technique. *Tellus A: Dynamic Meteorology and Oceanography*, 62(5), 591–604. <https://doi.org/10.1111/j.1600-0870.2010.00467.x>

Collins, Y., W., Rasch, P. J., Boville, B. A., McCaa, J., Williamson, D. L., Kiehl, J. T., Dai. (2004). Description of the NCAR Community Atmosphere Model (CAM 3.0) (No. NCAR/TN-464+STR). University Corporation for Atmospheric Research. *Вісник Харківського Національного Університету Імені В. Н. Каразіна. Серія «Біологія»*. <https://doi.org/doi:10.5065/D63N21CH>

Cuxart, J., Bougeault, P., & Redelsperger, J.-L. (2000). A turbulence scheme allowing for mesoscale and large-eddy simulations. *Q.J. Royal Met. Soc.*, 126(562), 1–30. <https://doi.org/10.1002/qj.49712656202>

Daniel, M., Lemonsu, A., Déqué, M., Somot, S., Alias, A., & Masson, V. (2019). Benefits of explicit urban parameterization in regional climate modeling to study climate and city interactions. *Climate Dynamics*, 52(5–6), 2745–2764. <https://doi.org/10.1007/s00382-018-4289-x>

De Ridder, K., & Schayes, G. (1997). The IAGL land surface model. *Journal of Applied Meteorology*, 36(2), 167–182. [https://doi.org/10.1175/1520-0450\(1997\)036<0167:tilsm>2.0.co;2](https://doi.org/10.1175/1520-0450(1997)036<0167:tilsm>2.0.co;2)

Decharme, B., Alkama, R., Douville, H., Becker, M., & Cazenave, A. (2010). Global Evaluation of the ISBA-TRIP Continental Hydrological System. Part II: Uncertainties in River Routing Simulation Related to Flow Velocity and Groundwater Storage. *Journal of Hydrometeorology*, 11(3), 601–617. <https://doi.org/10.1175/2010jhm1212.1>

Decharme, Bertrand, Delire, C., Minvielle, M., Colin, J., Vergnes, J.-P., Alias, A., Saint-Martin, D., Séférian, R., Sénési, S., & Voldoire, A. (2019). Recent Changes in the ISBA-CTRP Land Surface System for Use in the CNRM-CM6 Climate Model and in Global Off-Line Hydrological Applications. *J. Adv. Model. Earth Syst.*, 11(5), 1207–1252. <https://doi.org/10.1029/2018ms001545>

Dickinson, R E, Henderson-Sellers, A., & Kennedy, P. J. (1993). *Biosphere-Atmosphere Transfer Scheme (BATS) version 1e as coupled to the NCAR community climate model. Technical note. [NCAR (National Center for Atmospheric Research)]*. <https://www.osti.gov/biblio/5733868>



Dickinson, Robert E., Oleson, K. W., Bonan, G., Hoffman, F., Thornton, P., Vertenstein, M., Yang, Z.-L., & Zeng, X. (2006). The Community Land Model and Its Climate Statistics as a Component of the Community Climate System Model. *Journal of Climate*, 19(11), 2302–2324. <https://doi.org/10.1175/jcli3742.1>

Djurđević, V., & Rajković, B. (2008). Verification of a coupled atmosphere-ocean model using satellite observations over the Adriatic Sea. *Annales Geophysicae*, 26(7), 1935–1954. <https://doi.org/10.5194/angeo-26-1935-2008>

Douville, H., Planton, S., Royer, J.-F., Stephenson, D. B., Tyteca, S., Kergoat, L., Lafont, S., & Betts, R. A. (2000). Importance of vegetation feedbacks in doubled-CO₂ climate experiments. *J. Geophys. Res.*, 105(D11), 14841–14861. <https://doi.org/10.1029/1999jd901086>

Dudhia, J. (1989). Numerical Study of Convection Observed during the Winter Monsoon Experiment Using a Mesoscale Two-Dimensional Model. *J. Atmos. Sci.*, 46(20), 3077–3107. [https://doi.org/10.1175/1520-0469\(1989\)046<3077:nsocod>2.0.co;2](https://doi.org/10.1175/1520-0469(1989)046<3077:nsocod>2.0.co;2)

E van Meijgaard, A. S., LH van Ulft, WJ van de Berg, FC Bosveld, BJM van den Hurk, G. Lenderink. (2008). *The KNMI regional atmospheric climate model RACMO, version 2.1 KNMI number: TR-302, Year: 2008, Pages: 43.* <Https://www.knmi.nl/kennis-en-datacentrum/publicatie/the-knmi-regional-atmospheric-climate-model-racmo-version-2-1>.

ECMWF. (2003). IFS Documentation CY23R4—Part IV: Physical Processes. In P. White (Ed.), *IFS Documentation CY23R4*. ECMWF. <https://doi.org/10.21957/c11uegot3>

Ek, M. B., Mitchell, K. E., Lin, Y., Rogers, E., Grunmann, P., Koren, V., Gayno, G., & Tarpley, J. D. (2003). Implementation of Noah land surface model advances in the National Centers for Environmental Prediction operational mesoscale Eta model. *J. Geophys. Res.*, 108(D22). <https://doi.org/10.1029/2002jd003296>

Emanuel, K. A. (1991). A Scheme for Representing Cumulus Convection in Large-Scale Models. *J. Atmos. Sci.*, 48(21), 2313–2329. [https://doi.org/10.1175/1520-0469\(1991\)048<2313:asfrcc>2.0.co;2](https://doi.org/10.1175/1520-0469(1991)048<2313:asfrcc>2.0.co;2)

Ettema, J., van den Broeke, M. R., van Meijgaard, E., van de Berg, W. J., Box, J. E., & Steffen, K. (2010). Climate of the Greenland ice sheet using a high-resolution climate model – Part 1: Evaluation. *The Cryosphere*, 4(4), 511–527. <https://doi.org/10.5194/tc-4-511-2010>

Evans, J. P., Virgilio, G. D., Hirsch, A. L., Hoffmann, P., Remedio, A. R., Ji, F., Rockel, B., & Coppola, E. (2020). The CORDEX-Australasia ensemble: Evaluation and future projections. *Clim Dyn.* <https://doi.org/10.1007/s00382-020-05459-0>

Fels, S. B., & Schwarzkopf, M. D. (1975). The Simplified Exchange Approximation: A New Method for Radiative Transfer Calculations. *J. Atmos. Sci.*, 32(7), 1475–1488. [https://doi.org/10.1175/1520-0469\(1975\)032<1475:tseaan>2.0.co;2](https://doi.org/10.1175/1520-0469(1975)032<1475:tseaan>2.0.co;2)

Fouquart, Y., & Bonnel, B. (1980). Computations of solar heating of the earth's atmosphere: A new parameterization. *BEITR. PHYS. ATMOSPH.; DEU; DA. 1980; VOL. 53; NO 1; PP. 35-62; ABS. GER/FRE; BIBL. 2 P.*



Freidenreich, S. M., & Ramaswamy, V. (1999). A new multiple-band solar radiative parameterization for general circulation models. *J. Geophys. Res.*, 104(D24), 31389–31409. <https://doi.org/10.1029/1999jd900456>

Fritsch, J. M., & Chappell, C. F. (1980). Numerical Prediction of Convectively Driven Mesoscale Pressure Systems. Part I: Convective Parameterization. *J. Atmos. Sci.*, 37(8), 1722–1733. [https://doi.org/10.1175/1520-0469\(1980\)037<1722:npocdm>2.0.co;2](https://doi.org/10.1175/1520-0469(1980)037<1722:npocdm>2.0.co;2)

Gallée, H. (1995). Simulation of the Mesocyclonic Activity in the Ross Sea, Antarctica. *Mon. Wea. Rev.*, 123(7), 2051–2069. [https://doi.org/10.1175/1520-0493\(1995\)123<2051:sotmai>2.0.co;2](https://doi.org/10.1175/1520-0493(1995)123<2051:sotmai>2.0.co;2)

Gallée, H., & Duynkerke, P. G. (1997). Air-snow interactions and the surface energy and mass balance over the melting zone of west Greenland during the Greenland Ice Margin Experiment. *J. Geophys. Res.*, 102(D12), 13813–13824. <https://doi.org/10.1029/96jd03358>

Gallée, H., Guyomarc\textquotesingle, G., & Brun, E. (2001). Impact Of Snow Drift On The Antarctic Ice Sheet Surface Mass Balance: Possible Sensitivity To Snow-Surface Properties. *Boundary-Layer Meteorology*, 99(1), 1–19. <https://doi.org/10.1023/a:1018776422809>

Gallée, H., & Schayes, G. (1994). Development of a Three-Dimensional Meso-\$\upgamma\$ Primitive Equation Model: Katabatic Winds Simulation in the Area of Terra Nova Bay, Antarctica. *Mon. Wea. Rev.*, 122(4), 671–685. [https://doi.org/10.1175/1520-0493\(1994\)122<0671:doatdm>2.0.co;2](https://doi.org/10.1175/1520-0493(1994)122<0671:doatdm>2.0.co;2)

Geleyn, J.-F. (1988). Interpolation of wind, temperature and humidity values from model levels to the height of measurement. *Tellus A*, 40A(4), 347–351. <https://doi.org/10.1111/j.1600-0870.1988.tb00352.x>

Gerard, L., Piriou, J.-M., Brožková, R., Geleyn, J.-F., & Banciu, D. (2009). Cloud and Precipitation Parameterization in a Meso-Gamma-Scale Operational Weather Prediction Model. *Monthly Weather Review*, 137(11), 3960–3977. <https://doi.org/10.1175/2009mwr2750.1>

Giorgetta, M., M. A. ., & Wild. (1995). *The water vapour continuum and its representation in ECHAM4. Report / Max-Planck-Institut für Meteorologie*, 162. Cite as: [Http://hdl.handle.net/11858/00-001M-0000-0019-B569-F](http://hdl.handle.net/11858/00-001M-0000-0019-B569-F).

Giorgi, F., & Anyah, R. O. (2012). INTRODUCTION The road towards RegCM4 F. Giorgi1,\ast, R. O. Anyah2. *Clim. Res.*, 52, 3–6. <https://doi.org/10.3354/cr01089>

Giorgi, F., Coppola, E., Solmon, F., Mariotti, L., Sylla, M. B., Bi, X., Elguindi, N., Diro, G. T., Nair, V., Giuliani, G., Turuncoglu, U. U., Cozzini, S., Güttler, I., O'Brien, T. A., Tawfik, A. B., Shalaby, A., Zakey, A. S., Steiner, A. L., Stordal, F., ... Brankovic, C. (2012a). RegCM4: Model description and preliminary tests over multiple CORDEX domains. *Climate Research*, 52(1), 7–29. <https://doi.org/10.3354/cr01018>

Giorgi, F., Coppola, E., Solmon, F., Mariotti, L., Sylla, M. B., Bi, X., Elguindi, N., Diro, G. T., Nair, V., Giuliani, G., Turuncoglu, U. U., Cozzini, S., Güttler, I., O'Brien, T. A., Tawfik, A. B., Shalaby, A., Zakey, A. S., Steiner, A. L., Stordal, F., ... Brankovic, C. (2012b). RegCM4: Model description and preliminary tests over multiple CORDEX domains. *Clim. Res.*, 52, 7–29. <https://doi.org/10.3354/cr01018>

Giot, O., Termonia, P., Degrauwe, D., Troch, R. D., Caluwaerts, S., Smet, G., Berckmans, J., Deckmyn, A., Cruz, L. D., Meutter, P. D., Duerinckx, A., Gerard, L., Hamdi, R., Bergh, J. V. den, Ginderachter, M.



- V., & Schaebybroeck, B. V. (2016). Validation of the ALARO-0 model within the EURO-CORDEX framework. *Geosci. Model Dev.*, 9(3), 1143–1152. <https://doi.org/10.5194/gmd-9-1143-2016>
- Grell, G. A. (1993). Prognostic Evaluation of Assumptions Used by Cumulus Parameterizations. *Mon. Wea. Rev.*, 121(3), 764–787. [https://doi.org/10.1175/1520-0493\(1993\)121<0764:peoaub>2.0.co;2](https://doi.org/10.1175/1520-0493(1993)121<0764:peoaub>2.0.co;2)
- Guérémy, J. F. (2011). A continuous buoyancy based convection scheme: One-and three-dimensional validation. *Tellus A: Dynamic Meteorology and Oceanography*, 63(4), 687–706. <https://doi.org/10.1111/j.1600-0870.2011.00521.x>
- Haidvogel, D. B., Arango, H., Budgell, W. P., Cornuelle, B. D., Curchitser, E., Lorenzo, E. D., Fennel, K., Geyer, W. R., Hermann, A. J., Lanerolle, L., Levin, J., McWilliams, J. C., Miller, A. J., Moore, A. M., Powell, T. M., Shchepetkin, A. F., Sherwood, C. R., Signell, R. P., Warner, J. C., & Wilkin, J. (2008). Ocean forecasting in terrain-following coordinates: Formulation and skill assessment of the Regional Ocean Modeling System. *Journal of Computational Physics*, 227(7), 3595–3624. <https://doi.org/10.1016/j.jcp.2007.06.016>
- Han, J., & Pan, H.-L. (2011). Revision of Convection and Vertical Diffusion Schemes in the NCEP Global Forecast System. *Weather and Forecasting*, 26(4), 520–533. <https://doi.org/10.1175/waf-d-10-05038.1>
- Hoffmann, P., Katzfey, J. J., McGregor, J. L., & Thatcher, M. (2016). Bias and variance correction of sea surface temperatures used for dynamical downscaling. *J. Geophys. Res. Atmos.*, 121(21), 12,877–12,890. <https://doi.org/10.1002/2016jd025383>
- Holtslag, A. A. M., Bruijn, E. I. F. D., & Pan, H.-L. (1990). A High Resolution Air Mass Transformation Model for Short-Range Weather Forecasting. *Mon. Wea. Rev.*, 118(8), 1561–1575. [https://doi.org/10.1175/1520-0493\(1990\)118<1561:ahramt>2.0.co;2](https://doi.org/10.1175/1520-0493(1990)118<1561:ahramt>2.0.co;2)
- Hong, S.-Y., Dudhia, J., & Chen, S.-H. (2004). A Revised Approach to Ice Microphysical Processes for the Bulk Parameterization of Clouds and Precipitation. *Mon. Wea. Rev.*, 132(1), 103–120. [https://doi.org/10.1175/1520-0493\(2004\)132<0103:aratim>2.0.co;2](https://doi.org/10.1175/1520-0493(2004)132<0103:aratim>2.0.co;2)
- Hong, S.-Y., Noh, Y., & Dudhia, J. (2006). A New Vertical Diffusion Package with an Explicit Treatment of Entrainment Processes. *Monthly Weather Review*, 134(9), 2318–2341. <https://doi.org/10.1175/mwr3199.1>
- Hostetler, S. W., Giorgi, F., Bates, G. T., & Bartlein, P. J. (1994). Lake-atmosphere feedbacks associated with paleolakes Bonneville and Lahontan. *Science*, 263(5147), 665–668. <https://doi.org/10.1126/science.263.5147.665>
- Hourdin, F., Musat, I., Bony, S., Braconnot, P., Codron, F., Dufresne, J.-L., Fairhead, L., Filiberti, M.-A., Friedlingstein, P., Grandpeix, J.-Y., Krinner, G., LeVan, P., Li, Z.-X., & Lott, F. (2006). The LMDZ4 general circulation model: Climate performance and sensitivity to parametrized physics with emphasis on tropical convection. *Clim Dyn*, 27(7–8), 787–813. <https://doi.org/10.1007/s00382-006-0158-0>
- Hurk, B. J. J. van den, Viterbo, P., Beljaars, A., & Betts, A. (2000). Offline validation of the ERA40 surface scheme. 295. <https://doi.org/10.21957/9aoaspz8>



Hurley, P. (2007a). Modelling Mean and Turbulence Fields in the Dry Convective Boundary Layer with the Eddy-Diffusivity/Mass-Flux Approach. *Boundary-Layer Meteorol.*, 125(3), 525–536. <https://doi.org/10.1007/s10546-007-9203-8>

Hurley, P. (2007b). Modelling Mean and Turbulence Fields in the Dry Convective Boundary Layer with the Eddy-Diffusivity/Mass-Flux Approach. *Boundary-Layer Meteorol.*, 125(3), 525–536. <https://doi.org/10.1007/s10546-007-9203-8>

Iacono, M. J., Delamere, J. S., Mlawer, E. J., Shephard, M. W., Clough, S. A., & Collins, W. D. (2008). Radiative forcing by long-lived greenhouse gases: Calculations with the AER radiative transfer models. *J. Geophys. Res.*, 113(D13). <https://doi.org/10.1029/2008jd009944>

Jacob, D. (2001). A note to the simulation of the annual and inter-annual variability of the water budget over the Baltic Sea drainage basin. *Meteorology and Atmospheric Physics*, 77(1–4), 61–73. <https://doi.org/10.1007/s007030170017>

Jacob, D., & Podzun, R. (1997). Sensitivity studies with the regional climate model REMO. *Meteorol. Atmos. Phys.*, 63(1–2), 119–129. <https://doi.org/10.1007/bf01025368>

Janjić, Z. I. (1994). The Step-Mountain Eta Coordinate Model: Further Developments of the Convection, Viscous Sublayer, and Turbulence Closure Schemes. *Mon. Wea. Rev.*, 122(5), 927–945. [https://doi.org/10.1175/1520-0493\(1994\)122<0927:tsmecm>2.0.co;2](https://doi.org/10.1175/1520-0493(1994)122<0927:tsmecm>2.0.co;2)

Janjic, Z. I. (2003). A nonhydrostatic model based on a new approach. *Meteorology and Atmospheric Physics*, 82(1–4), 271–285. <https://doi.org/10.1007/s00703-001-0587-6>

Jiao, Y., & Jones, C. (2008). Comparison Studies of Cloud- and Convection-Related Processes Simulated by the Canadian Regional Climate Model over the Pacific Ocean. *Monthly Weather Review*, 136(11), 4168–4187. <https://doi.org/10.1175/mwr2494.1>

Jonathan Beuvier, et al., Cindy Lebeaupin Brossier, Karine Béranger, Thomas Arsouze, Romain Bourdalle-Badie. (2012). MED12, OCEANIC COMPONENT FOR THE MODELING OF THE REGIONAL MEDITERRANEAN EARTH SYSTEM. *Mercator Ocean Quarterly Newsletter*, #46. 2012.<hal-01138958>.

Kain, J. S. (2004). The Kain–Fritsch Convective Parameterization: An Update. *J. Appl. Meteor.*, 43(1), 170–181. [https://doi.org/10.1175/1520-0450\(2004\)043<0170:tkcpau>2.0.co;2](https://doi.org/10.1175/1520-0450(2004)043<0170:tkcpau>2.0.co;2)

Kain, J. S., & Fritsch, J. M. (1990). A One-Dimensional Entrainment/Detraining Plume Model and Its Application in Convective Parameterization. *J. Atmos. Sci.*, 47(23), 2784–2802. [https://doi.org/10.1175/1520-0469\(1990\)047<2784:aodepm>2.0.co;2](https://doi.org/10.1175/1520-0469(1990)047<2784:aodepm>2.0.co;2)

Kiehl, J. T., Hack, J. J., Bonan, G. B., Boville, B. A., Williamson, D. L., & Rasch, P. J. (1998). The National Center for Atmospheric Research Community Climate Model: CCM3\ast. *J. Climate*, 11(6), 1131–1149. [https://doi.org/10.1175/1520-0442\(1998\)011<1131:tncfar>2.0.co;2](https://doi.org/10.1175/1520-0442(1998)011<1131:tncfar>2.0.co;2)

Kiehl, P. J., J. T. ,. Hack, J. J. ,. Bonan, G. B. ,. Boville, B. A. ,. Briegleb, B. P. ,. Williamson, D. L. ,. & Rasch. (1996). *Description of the NCAR Community Climate Model (CCM3) ##(No. NCAR/TN-420+STR)*. University Corporation for Atmospheric Research. <https://doi.org/10.5065/D6FF3Q99>



Kinne, S., Schulz, M., Textor, C., Guibert, S., Balkanski, Y., Bauer, S. E., Berntsen, T., Berglen, T. F., Boucher, O., Chin, M., Collins, W., Dentener, F., Diehl, T., Easter, R., Feichter, J., Fillmore, D., Ghan, S., Ginoux, P., Gong, S., ... Tie, X. (2006). An AeroCom initial assessment – optical properties in aerosol component modules of global models. *Atmos. Chem. Phys.*, 6(7), 1815–1834. <https://doi.org/10.5194/acp-6-1815-2006>

Kittel, C., Amory, C., Agosta, C., Jourdain, N. C., Hofer, S., Delhasse, A., Doutreloup, S., Huot, P.-V., Lang, C., Fichefet, T., & Fettweis, X. (2021). Diverging future surface mass balance between the Antarctic ice shelves and grounded ice sheet. *The Cryosphere*, 15(3), 1215–1236. <https://doi.org/10.5194/tc-15-1215-2021>

Klemp, J. B., Dudhia, J., & Hassiotis, A. D. (2008). An Upper Gravity-Wave Absorbing Layer for NWP Applications. *Mon. Wea. Rev.*, 136(10), 3987–4004. <https://doi.org/10.1175/2008mwr2596.1>

Kowalczyk, E., Stevens, L., Law, R., Dix, M., Wang, Y., Harman, I., Haynes, K., Srbinovsky, J., Pak, B., & Ziehn, T. (2013). The land surface model component of ACCESS: description and impact on the simulated surface climatology. *A*, 63(1), 65–82. <https://doi.org/10.22499/2.6301.005>

Krži, A., Tošić, I., Djurdjević, V., Veljović, K., & Rajković, B. (2011). Changes in climate indices for Serbia according to the SRES-A1B and SRES-A2 scenarios. *Climate Research*, 49(1), 73–86. <https://doi.org/10.3354/cr01008>

KUO, H. L. (1965). Further studies of the properties of cellular convection in a conditionally unstable atmosphere. *Tellus*, 17(4), 413–433. <https://doi.org/10.1111/j.2153-3490.1965.tb00204.x>

Lacis, A. A., & Hansen, J. E. (1974). A parameterization for the absorption of solar radiation in the Earth's atmosphere. *J. Atmos. Sci.*, 31, 118–133. [https://doi.org/10.1175/1520-0469\(1974\)031%3C0118%3AAPFTAO%3E2.0.CO;2](https://doi.org/10.1175/1520-0469(1974)031%3C0118%3AAPFTAO%3E2.0.CO;2)

Lamarque, Jean-François, McConnell, J. R., Shindell, D. T., Orlando, J. J., & Tyndall, G. S. (2011). Understanding the drivers for the 20th century change of hydrogen peroxide in Antarctic ice-cores. *Geophysical Research Letters*, 38(4). <https://doi.org/10.1029/2010GL045992>

Lamarque, J.-F., Bond, T. C., Eyring, V., Granier, C., Heil, A., Klimont, Z., Lee, D., Lioussse, C., Mieville, A., Owen, B., Schultz, M. G., Shindell, D., Smith, S. J., Stehfest, E., Aardenne, J. V., Cooper, O. R., Kainuma, M., Mahowald, N., McConnell, J. R., ... Vuuren, D. P. van. (2010). Historical (1850–2000) gridded anthropogenic and biomass burning emissions of reactive gases and aerosols: Methodology and application. *Atmos. Chem. Phys.*, 10(15), 7017–7039. <https://doi.org/10.5194/acp-10-7017-2010>

Lefebre, F. (2003). Modeling of snow and ice melt at ETH Camp (West Greenland): A study of surface albedo. *J. Geophys. Res.*, 108(D8). <https://doi.org/10.1029/2001jd001160>

Lenaerts, J. T. M., Broeke, M. R. van den, Déry, S. J., Meijgaard, E. van, Berg, W. J. van de, Palm, S. P., & Rodrigo, J. S. (2012). Modeling drifting snow in Antarctica with a regional climate model: 1. Methods and model evaluation. *J. Geophys. Res.*, 117(D5), n/a-n/a. <https://doi.org/10.1029/2011jd016145>

Lenderink, G., & Holtslag, A. A. M. (2004). An updated length-scale formulation for turbulent mixing in clear and cloudy boundary layers. *Q. J. R. Meteorol. Soc.*, 130(604), 3405–3427. <https://doi.org/10.1256/qj.03.117>



- Leutwyler, D., Lüthi, D., Ban, N., Fuhrer, O., & Schär, C. (2017). Evaluation of the convection-resolving climate modeling approach on continental scales. *J. Geophys. Res. Atmos.*, 122(10), 5237–5258. <https://doi.org/10.1002/2016jd026013>
- L'Hévéder, B., Li, L., Sevault, F., & Somot, S. (2013). Interannual variability of deep convection in the Northwestern Mediterranean simulated with a coupled AORCM. *Climate Dynamics*, 41(3–4), 937–960. <https://doi.org/10.1007/s00382-012-1527-5>
- L'Hévéder, Blandine, Li, L., Sevault, F., & Somot, S. (2012). Interannual variability of deep convection in the Northwestern Mediterranean simulated with a coupled AORCM. *Clim Dyn*, 41(3–4), 937–960. <https://doi.org/10.1007/s00382-012-1527-5>
- Li, D., Yin, B., Feng, J., Dosio, A., Geyer, B., Qi, J., Shi, H., & Xu, Z. (2018). Present Climate Evaluation and Added Value Analysis of Dynamically Downscaled Simulations of CORDEX—East Asia. *Journal of Applied Meteorology and Climatology*, 57(10), 2317–2341. <https://doi.org/10.1175/jamc-d-18-0008.1>
- Li, J., & Barker, H. W. (2005). A Radiation Algorithm with Correlated-k Distribution. Part I: Local Thermal Equilibrium. *Journal of the Atmospheric Sciences*, 62(2), 286–309. <https://doi.org/10.1175/jas-3396.1>
- Li, Z.-X. (1999). Ensemble Atmospheric GCM Simulation of Climate Interannual Variability from 1979 to 1994. *J. Climate*, 12(4), 986–1001. [https://doi.org/10.1175/1520-0442\(1999\)012<0986:eagsoc>2.0.co;2](https://doi.org/10.1175/1520-0442(1999)012<0986:eagsoc>2.0.co;2)
- Lim, K.-S. S., & Hong, S.-Y. (2010). Development of an Effective Double-Moment Cloud Microphysics Scheme with Prognostic Cloud Condensation Nuclei (CCN) for Weather and Climate Models. *Monthly Weather Review*, 138(5), 1587–1612. <https://doi.org/10.1175/2009mwr2968.1>
- Lin, Y.-L., Farley, R. D., & Orville, H. D. (1983). Bulk Parameterization of the Snow Field in a Cloud Model. *J. Climate Appl. Meteor.*, 22(6), 1065–1092. [https://doi.org/10.1175/1520-0450\(1983\)022<1065:bpotsf>2.0.co;2](https://doi.org/10.1175/1520-0450(1983)022<1065:bpotsf>2.0.co;2)
- Lipson, M. J., Thatcher, M., Hart, M. A., & Pitman, A. (2018). A building energy demand and urban land surface model. *Q.J.R. Meteorol. Soc.*, 144(714), 1572–1590. <https://doi.org/10.1002/qj.3317>
- Lopez, P. (2002). Implementation and validation of a new prognostic large-scale cloud and precipitation scheme for climate and data-assimilation purposes. *Q. J. R. Meteorol. Soc.*, 128(579), 229–257. <https://doi.org/10.1256/00359000260498879>
- Lott, F. (1999). Alleviation of Stationary Biases in a GCM through a Mountain Drag Parameterization Scheme and a Simple Representation of Mountain Lift Forces. *Mon. Wea. Rev.*, 127(5), 788–801. [https://doi.org/10.1175/1520-0493\(1999\)127<0788:aosbia>2.0.co;2](https://doi.org/10.1175/1520-0493(1999)127<0788:aosbia>2.0.co;2)
- Lott, F., & Miller, M. J. (1997). A new subgrid-scale orographic drag parametrization: Its formulation and testing. *Q.J Royal Met. Soc.*, 123(537), 101–127. <https://doi.org/10.1002/qj.49712353704>
- Louis, J.-F. (1979). A parametric model of vertical eddy fluxes in the atmosphere. *Boundary-Layer Meteorology*, 17(2), 187–202. <https://doi.org/10.1007/BF00117978>



Martynov, A., Laprise, R., Sushama, L., Winger, K., Šeparović, L., & Dugas, B. (2013). Reanalysis-driven climate simulation over CORDEX North America domain using the Canadian Regional Climate Model, version 5: Model performance evaluation. *Clim Dyn*, 41(11–12), 2973–3005. <https://doi.org/10.1007/s00382-013-1778-9>

McCaa, J. R., & Bretherton, C. S. (2004). A new parameterization for shallow cumulus convection and its application to marine subtropical cloud-topped boundary layers. Part II: Regional simulations of marine boundary layer clouds. *Monthly Weather Review*, 132(4), 883–896. [https://doi.org/10.1175/1520-0493\(2004\)132<0883:ANPFSC>2.0.CO;2](https://doi.org/10.1175/1520-0493(2004)132<0883:ANPFSC>2.0.CO;2)

McGregor, J. L. (2003). *A new convection scheme using simple closure*. In: Meighen, P. J.; Hollis, A. J. editors, editor/s. *Current issues in the parameterization of convection: Extended abstracts of presentations at the fifteenth annual BMRC Modelling Workshop*; Melbourne; Bureau of Meteorology Research Centre. Melbourne, Vic.: BMRC; 33-36. <Http://hdl.handle.net/102.100.100/194317?index=1>.

Mearns, et al., L. O. (2017). *The NA-CORDEX dataset, version 1.0*. NCAR Climate Data Gateway, Boulder CO, accessed [date]. <https://doi.org/10.5065/D6SJ1JCH>

Meinshausen, M., Vogel, E., Nauels, A., Lorbacher, K., Meinshausen, N., Etheridge, D. M., Fraser, P. J., Montzka, S. A., Rayner, P. J., Trudinger, C. M., Krummel, P. B., Beyerle, U., Canadell, J. G., Daniel, J. S., Enting, I. G., Law, R. M., Lunder, C. R., O{textquotesingle}Doherty, S., Prinn, R. G., ... Weiss, R. (2017). Historical greenhouse gas concentrations for climate modelling (CMIP6). *Geosci. Model Dev.*, 10(5), 2057–2116. <https://doi.org/10.5194/gmd-10-2057-2017>

Meleshko, O., Korshunov, O., & Шабанов, Д. (2014). The study of three hemiclonal population systems of Pelophylax esculentus complex from the Seversko-Donetskiy center of green frogs' diversity. *Вісник Харківського Національного Університету Імені В. Н. Каразіна. Серія «Біологія»*, 1100, 153–158.

Mesinger, F., Janjić, Z. I., Ničković, S., Gavrilov, D., & Deaven, D. G. (1988). The Step-Mountain Coordinate: Model Description and Performance for Cases of Alpine Lee Cyclogenesis and for a Case of an Appalachian Redevelopment. *Mon. Wea. Rev.*, 116(7), 1493–1518. [https://doi.org/10.1175/1520-0493\(1988\)116<1493:tsmcmd>2.0.co;2](https://doi.org/10.1175/1520-0493(1988)116<1493:tsmcmd>2.0.co;2)

Mironov, D., Heise, E., Kourzeneva, E., Ritter, B., Schneider, N., & Terzhevik, A. (2010a). Implementation of the lake parameterisation scheme FLake into the numerical weather prediction model COSMO. *Boreal Environment Research*, 15(2), 218–230.

Mironov, D., Heise, E., Kourzeneva, E., Ritter, B., Schneider, N., & Terzhevik, A. (2010b). Implementation of the lake parameterisation scheme FLake into the numerical weather prediction model COSMO. *Boreal Environment Research*, 15(2), 218–230.

Mlawer, E. J., Taubman, S. J., Brown, P. D., Iacono, M. J., & Clough, S. A. (1997). Radiative transfer for inhomogeneous atmospheres: RRTM, a validated correlated-k model for the longwave. *J. Geophys. Res.*, 102(D14), 16663–16682. <https://doi.org/10.1029/97jd00237>

Moigne, P. L., Colin, J., & Decharme, B. (2016a). Impact of lake surface temperatures simulated by the FLake scheme in the CNRM-CM5 climate model. *Tellus A: Dynamic Meteorology and Oceanography*, 68(1), 31274. <https://doi.org/10.3402/tellusa.v68.31274>



- Moigne, P. L., Colin, J., & Decharme, B. (2016b). Impact of lake surface temperatures simulated by the FLake scheme in the CNRM-CM5 climate model. *Tellus A: Dynamic Meteorology and Oceanography*, 68(1), 31274. <https://doi.org/10.3402/tellusa.v68.31274>
- Morcrette, Jean-Jacques. (1990). Impact of Changes to the Radiation Transfer Parameterizations Plus Cloud Optical Properties in the ECMWF Model. *Mon. Wea. Rev.*, 118(4), 847–873. [https://doi.org/10.1175/1520-0493\(1990\)118<847:iocctr>2.0.co;2](https://doi.org/10.1175/1520-0493(1990)118<847:iocctr>2.0.co;2)
- Morcrette, Jean-Jacques. (2002). The Surface Downward Longwave Radiation in the ECMWF Forecast System. *J. Climate*, 15(14), 1875–1892. [https://doi.org/10.1175/1520-0442\(2002\)015<1875:tsdlri>2.0.co;2](https://doi.org/10.1175/1520-0442(2002)015<1875:tsdlri>2.0.co;2)
- Morcrette, Jean-Jacques, Smith, L., & Fouquart, Y. (1986). Pressure and temperature dependence of the absorption in longwave radiation parameterizations. *Beitraege Zur Physik Der Atmosphaere (ISSN 0005-8173*, 59, 455–469.
- Morcrette, J.-J., Barker, H. W., Cole, J. N. S., Iacono, M. J., & Pincus, R. (2008). Impact of a New Radiation Package, McRad, in the ECMWF Integrated Forecasting System. *Monthly Weather Review*, 136(12), 4773–4798. <https://doi.org/10.1175/2008mwr2363.1>
- Morrison, H., McCoy, R. B., Klein, S. A., Xie, S., Luo, Y., Avramov, A., Chen, M., Cole, J. N. S., Falk, M., Foster, M. J., del Genio, A. D., Harrington, J. Y., Hoose, C., Khairoutdinov, M. F., Larson, V. E., Liu, X., McFarquhar, G. M., Poellot, M. R., von Salzen, K., ... Zhang, G. (2009). Intercomparison of model simulations of mixed-phase clouds observed during the ARM Mixed-Phase Arctic Cloud Experiment. II: Multilayer cloud. *Quarterly Journal of the Royal Meteorological Society*, 135(641), 1003–1019. <https://doi.org/10.1002/qj.415>
- Munneke, P. K., Broeke, M. R. van den, Lenaerts, J. T. M., Flanner, M. G., Gardner, A. S., & Berg, W. J. van de. (2011). A new albedo parameterization for use in climate models over the Antarctic ice sheet. *J. Geophys. Res.*, 116(D5). <https://doi.org/10.1029/2010jd015113>
- Nabat, P., Somot, S., Cassou, C., Mallet, M., Michou, M., Bouniol, D., Decharme, B., Drugé, T., Roehrig, R., & Saint-Martin, D. (2020). Modulation of radiative aerosols effects by atmospheric circulation over the Euro-Mediterranean region. *Atmos. Chem. Phys.*, 20(14), 8315–8349. <https://doi.org/10.5194/acp-20-8315-2020>
- Nakanishi, M., & Niino, H. (2004). An improved Mellor-Yamada Level-3 model with condensation physics: Its design and verification. *Boundary-Layer Meteorology*, 112(1), 1–31. <https://doi.org/10.1023/B:BOUN.0000020164.04146.98>
- Neggers, R. A. J., Köhler, M., & Beljaars, A. C. M. (2009). A Dual Mass Flux Framework for Boundary Layer Convection. Part I: Transport. *Journal of the Atmospheric Sciences*, 66(6), 1465–1487. <https://doi.org/10.1175/2008jas2635.1>
- Niu, G.-Y., Yang, Z.-L., Mitchell, K. E., Chen, F., Ek, M. B., Barlage, M., Kumar, A., Manning, K., Niyogi, D., Rosero, E., Tewari, M., & Xia, Y. (2011). The community Noah land surface model with multiparameterization options (Noah-MP): 1. Model description and evaluation with local-scale measurements. *J. Geophys. Res.*, 116(D12). <https://doi.org/10.1029/2010jd015139>



Noilhan, J., & Mahfouf, J.-F. (1996). The ISBA land surface parameterisation scheme. *Global and Planetary Change*, 13(1–4), 145–159. [https://doi.org/10.1016/0921-8181\(95\)00043-7](https://doi.org/10.1016/0921-8181(95)00043-7)

Nordeng, T.-E. (1994). Extended versions of the convective parametrization scheme at ECMWF and their impact on the mean and transient activity of the model in the tropics. 206, 41. <https://doi.org/10.21957/e34xwhysw>

Oki, T., & Sud, Y. C. (1998). Design of Total Runoff Integrating Pathways (TRIP)—A Global River Channel Network. *Earth Interactions*, 2(1), 1–37. [https://doi.org/10.1175/1087-3562\(1998\)002<0001:DOTRIP>2.3.CO;2](https://doi.org/10.1175/1087-3562(1998)002<0001:DOTRIP>2.3.CO;2)

Ozturk, T., Turp, M. T., Türkeş, M., & Kurnaz, M. L. (2017). Projected changes in temperature and precipitation climatology of Central Asia CORDEX Region 8 by using RegCM4.3.5. *Atmospheric Research*, 183, 296–307. <https://doi.org/10.1016/j.atmosres.2016.09.008>

Ozturk, T., Turp, M. T., Türkeş, M., & Kurnaz, M. L. (2018). Future projections of temperature and precipitation climatology for CORDEX-MENA domain using RegCM4.4. *Atmospheric Research*, 206, 87–107. <https://doi.org/10.1016/j.atmosres.2018.02.009>

Pal, J. S., Giorgi, F., Bi, X., Elguindi, N., Solmon, F., Gao, X., Rauscher, S. A., Francisco, R., Zakey, A., Winter, J., Ashfaq, M., Syed, F. S., Bell, J. L., Diffenbaugh, N. S., Karmacharya, J., Konaré, A., Martinez, D., Rocha, R. P. da, Sloan, L. C., & Steiner, A. L. (2007). Regional Climate Modeling for the Developing World: The ICTP RegCM3 and RegCNET. *Bulletin of the American Meteorological Society*, 88(9), 1395–1410. <https://doi.org/10.1175/bams-88-9-1395>

Pal, J. S., Small, E. E., & Eltahir, E. A. B. (2000). Simulation of regional-scale water and energy budgets: Representation of subgrid cloud and precipitation processes within RegCM. *J. Geophys. Res.*, 105(D24), 29579–29594. <https://doi.org/10.1029/2000jd900415>

Panitz, H.-J., Dosio, A., Büchner, M., Lüthi, D., & Keuler, K. (2013). COSMO-CLM (CCLM) climate simulations over CORDEX-Africa domain: Analysis of the ERA-Interim driven simulations at 0.44° and 0.22° resolution. *Clim Dyn*, 42(11–12), 3015–3038. <https://doi.org/10.1007/s00382-013-1834-5>

Per Undén, A. T., Laura Rontu, Heikki Järvinen, Peter Lynch, Javier Calvo, Gerard Cats, Joan Cuxart, Kalle Eerola, Carl Fortelius, Jose Antonio Garcia-Moya, Colin Jones, Geert Lenderlink, Aidan McDonald, Ray McGrath, Beatriz Navascues, Niels Woetman Nielsen, Viel Ødegaard, Ernesto Rodriguez, Markku Rummukainen, Rein Room, Kai Sattler, Bent Hansen Sass, Hannu Savijärvi, Ben Wickers Schreur, Robert Sigg, Han The. (2002). *HIRLAM-5 Scientific Documentation*. HIRLAM-5 Project, c/o Per Undén SMHI, S-601 76 Norrköping, SWEDEN. http://www.hirlam.org/index.php/hirlam-documentation/doc_download/308-unden-et-al-2002.

Piriou, J.-M., Redelsperger, J.-L., Geleyn, J.-F., Lafore, J.-P., & Guichard, F. (2007). An Approach for Convective Parameterization with Memory: Separating Microphysics and Transport in Grid-Scale Equations. *Journal of the Atmospheric Sciences*, 64(11), 4127–4139. <https://doi.org/10.1175/2007jas2144.1>

Powers, J. G., Klemp, J. B., Skamarock, W. C., Davis, C. A., Dudhia, J., Gill, D. O., Coen, J. L., Gochis, D. J., Ahmadov, R., Peckham, S. E., Grell, G. A., Michalakes, J., Trahan, S., Benjamin, S. G., Alexander, C. R., Dimego, G. J., Wang, W., Schwartz, C. S., Romine, G. S., ... Duda, M. G. (2017). The Weather



Research and Forecasting Model: Overview, System Efforts, and Future Directions. *Bulletin of the American Meteorological Society*, 98(8), 1717–1737. <https://doi.org/10.1175/bams-d-15-00308.1>

Räisänen, M., P., Rummukainen, & Räisänen, J. (2000). *Modification of the HIRLAM radiation scheme for use in the Rossby Centre regional atmospheric climate model*. Department of Meteorology, University of Helsinki, 49, p. 71.

Rasch, P. J., & Kristjánsson, J. E. (1998). A Comparison of the CCM3 Model Climate Using Diagnosed and Predicted Condensate Parameterizations. *J. Climate*, 11(7), 1587–1614. [https://doi.org/10.1175/1520-0442\(1998\)011<1587:acotcm>2.0.co;2](https://doi.org/10.1175/1520-0442(1998)011<1587:acotcm>2.0.co;2)

Raschendorfer, M. (2001). *The new turbulence parameterization of LM*. COSMO Newsletter, No. 1, Consortium for Small-Scale Modeling, Offenbach, Germany, 89–98, http://www.cosmo-model.org/content/model/documentation/newsLetters/newsLetter01/newsLetter_01.pdf.

Raschendorfer, M. (2008). *Revision of the Turbulent Gust Diagnostics in the COSMO Model*. COSMO News letter, 8, 17–22. (Available at: www.cosmo-model.org).

Rechid, D., Raddatz, T. J., & Jacob, D. (2008). Parameterization of snow-free land surface albedo as a function of vegetation phenology based on MODIS data and applied in climate modelling. *Theor Appl Climatol*, 95(3–4), 245–255. <https://doi.org/10.1007/s00704-008-0003-y>

Ricard, J. L., & Royer, J. F. (1993). A statistical cloud scheme for use in an AGCM. *Annales Geophysicae*, 11, 1095–1115.

Ridder, K. D. (1997). Radiative Transfer in the IAGL Land Surface Model. *J. Appl. Meteor.*, 36(1), 12–21. [https://doi.org/10.1175/1520-0450\(1997\)036<0012:rtilt>2.0.co;2](https://doi.org/10.1175/1520-0450(1997)036<0012:rtilt>2.0.co;2)

Ritter, B., & Geleyn, J.-F. (1992). A Comprehensive Radiation Scheme for Numerical Weather Prediction Models with Potential Applications in Climate Simulations. *Mon. Wea. Rev.*, 120(2), 303–325. [https://doi.org/10.1175/1520-0493\(1992\)120<0303:acrfsn>2.0.co;2](https://doi.org/10.1175/1520-0493(1992)120<0303:acrfsn>2.0.co;2)

Rotstain, L. D., Collier, M. A., Mitchell, R. M., Qin, Y., Campbell, S. K., & Dravitzki, S. M. (2011). Simulated enhancement of ENSO-related rainfall variability due to Australian dust. *Atmos. Chem. Phys.*, 11(13), 6575–6592. <https://doi.org/10.5194/acp-11-6575-2011>

Rotstain, Leon D. (1997). A physically based scheme for the treatment of stratiform clouds and precipitation in large-scale models. I: Description and evaluation of the microphysical processes. *Q.J Royal Met. Soc.*, 123(541), 1227–1282. <https://doi.org/10.1002/qj.49712354106>

Rotstain, Leon D., & Lohmann, U. (2002). Simulation of the tropospheric sulfur cycle in a global model with a physically based cloud scheme. *J. Geophys. Res.*, 107(D21), AAC 20-1-AAC 20-21. <https://doi.org/10.1029/2002jd002128>

Ruti, P. M., Somot, S., Giorgi, F., Dubois, C., Flaounas, E., Obermann, A., Dell'Aquila, A., Pisacane, G., Harzallah, A., Lombardi, E., Ahrens, B., Akhtar, N., Alias, A., Arsouze, T., Aznar, R., Bastin, S., Bartholy, J., Béranger, K., Beuvier, J., ... Vervatis, V. (2016). Med-CORDEX Initiative for Mediterranean Climate Studies. *Bulletin of the American Meteorological Society*, 97(7), 1187–1208. <https://doi.org/10.1175/bams-d-14-00176.1>



Samuelsson, W. J., P. ., Gollvik, S. ., Kupiainen, M. ., Kourzeneva, E. ., & van de Berg. (2015). *The surface processes of the Rossby Centre regional atmospheric climate model (RCA4)*. Retrieved from SMHI website: <Http://urn.kb.se/resolve?urn=urn:nbn:se:smhi:diva-2840>.

Sandvik, A.D. (1998). Implementation and validation of a condensation scheme in a nonhydrostatic mesoscale model. *Monthly Weather Review*, 126(7), 1882–1905. [https://doi.org/10.1175/1520-0493\(1998\)126<1882:iavoac>2.0.co;2](https://doi.org/10.1175/1520-0493(1998)126<1882:IAVOAC>2.0.CO;2)

Sandvik, Anne Dagrun. (1998). Implementation and Validation of a Condensation Scheme in a Nonhydrostatic Mesoscale Model. *Mon. Wea. Rev.*, 126(7), 1882–1905. [https://doi.org/10.1175/1520-0493\(1998\)126<1882:iavoac>2.0.co;2](https://doi.org/10.1175/1520-0493(1998)126<1882:iavoac>2.0.co;2)

Sanjay, J., Revadekar, J. V., Ramarao, M. V. S., Borgaonkar, H., Sengupta, S., Kothawale, D. R., Patel, J., Mahesh, R., Ingle, S., AchutaRao, K., Srivastava, A. K., & Ratnam, J. V. (2020). Temperature Changes in India. In *Assessment of Climate Change over the Indian Region* (pp. 21–45). Springer Singapore. https://doi.org/10.1007/978-981-15-4327-2_2

Sanjay, Jayanarayanan, Krishnan, R., Shrestha, A. B., Rajbhandari, R., & Ren, G.-Y. (2017). Downscaled climate change projections for the Hindu Kush Himalayan region using CORDEX South Asia regional climate models. *Advances in Climate Change Research*, 8(3), 185–198. <https://doi.org/10.1016/j.accre.2017.08.003>

Sannino, G., Herrmann, M., Carillo, A., Rupolo, V., Ruggiero, V., Artale, V., & Heimbach, P. (2009). An eddy-permitting model of the Mediterranean Sea with a two-way grid refinement at the Strait of Gibraltar. *Ocean Modelling*, 30(1), 56–72. <https://doi.org/10.1016/j.ocemod.2009.06.002>

Savijärvi, H. (1990). Fast Radiation Parameterization Schemes for Mesoscale and Short-Range Forecast Models. *J. Appl. Meteor.*, 29(6), 437–447. [https://doi.org/10.1175/1520-0450\(1990\)029<0437:frpsfm>2.0.co;2](https://doi.org/10.1175/1520-0450(1990)029<0437:frpsfm>2.0.co;2)

Schlemmer, L., Schär, C., Lüthi, D., & Strelbel, L. (2018). A Groundwater and Runoff Formulation for Weather and Climate Models. *J. Adv. Model. Earth Syst.*, 10(8), 1809–1832. <https://doi.org/10.1029/2017ms001260>

Schrodin, E., & E. Heise, 2002. (2002). A New Multi-Layer Soil Model. *COSMO Newsletter No.2*, 149–151.

Schwarzkopf, M. D., & Ramaswamy, V. (1999). Radiative effects of CH₄, N₂O, halocarbons and the foreign-broadened H₂O continuum: A GCM experiment. *J. Geophys. Res.*, 104(D8), 9467–9488. <https://doi.org/10.1029/1999jd900003>

Scinocca, J. F., Kharin, V. V., Jiao, Y., Qian, M. W., Lazare, M., Solheim, L., Flato, G. M., Biner, S., Desgagne, M., & Dugas, B. (2015). Coordinated Global and Regional Climate Modeling\ast. *Journal of Climate*, 29(1), 17–35. <https://doi.org/10.1175/jcli-d-15-0161.1>

Seifert, A., & Beheng, K. D. (2001). A double-moment parameterization for simulating autoconversion, accretion and selfcollection. *Atmospheric Research*, 59–60, 265–281. [https://doi.org/10.1016/S0169-8095\(01\)00126-0](https://doi.org/10.1016/S0169-8095(01)00126-0)



Seifert, A., & Beheng, K. D. (2005). A two-moment cloud microphysics parameterization for mixed-phase clouds. Part 1: Model description. *Meteorol. Atmos. Phys.*, 92(1–2), 45–66. <https://doi.org/10.1007/s00703-005-0112-4>

Sein, D. V., Mikolajewicz, U., Gröger, M., Fast, I., Cabos, W., Pinto, J. G., Hagemann, S., Semmler, T., Izquierdo, A., & Jacob, D. (2015). Regionally coupled atmosphere-ocean-sea ice-marine biogeochemistry model ROM: 1. Description and validation. *J. Adv. Model. Earth Syst.*, 7(1), 268–304. <https://doi.org/10.1002/2014ms000357>

Šeparović, L., Alexandru, A., Laprise, R., Martynov, A., Sushama, L., Winger, K., Tete, K., & Valin, M. (2013). Present climate and climate change over North America as simulated by the fifth-generation Canadian regional climate model. *Clim Dyn*, 41(11–12), 3167–3201. <https://doi.org/10.1007/s00382-013-1737-5>

Sevault, F., Somot, S., Alias, A., Dubois, C., Lebeaupin-Brossier, C., Nabat, P., Adloff, F., Déqué, M., & Decharme, B. (2014). A fully coupled Mediterranean regional climate system model: Design and evaluation of the ocean component for the 1980–2012 period. *Tellus A: Dynamic Meteorology and Oceanography*, 66(1), 23967. <https://doi.org/10.3402/tellusa.v66.23967>

Shkolnik, I. M., & Efimov, S. V. (2013). Cyclonic activity in high latitudes as simulated by a regional atmospheric climate model: Added value and uncertainties. *Environ. Res. Lett.*, 8(4), 045007. <https://doi.org/10.1088/1748-9326/8/4/045007>

Shkolnik, I. M., Nadyozhina, E. D., Pavlova, T. V., Molkentin, E. K., & Semioshina, A. A. (2010). Snow cover and permafrost evolution in Siberia as simulated by the MGO regional climate model in the 20th and 21st centuries. *Environ. Res. Lett.*, 5(1), 015005. <https://doi.org/10.1088/1748-9326/5/1/015005>

Shneerov, B. E., Shneerov, B. E., Shneerov, B. E., Shneerov, B. E. (2001). *Current state of MGO general circulation model (version MGO-2)* MGO Proc. pp 3–43.

Siebesma, A. P., Soares, P. M. M., & Teixeira, J. (2007). A Combined Eddy-Diffusivity Mass-Flux Approach for the Convective Boundary Layer. *Journal of the Atmospheric Sciences*, 64(4), 1230–1248. <https://doi.org/10.1175/jas3888.1>

Skamarock, J. G., W. C., Klemp, J. B., Dudhia, J., Gill, D. O., Barker, D., Duda, M. G., Powers. (2008). *A Description of the #Advanced Research WRF Version 3 (No. NCAR/TN-475+STR)*. University Corporation for Atmospheric Research. <https://doi.org/10.5065/D68S4MVH>

Smith, R. N. B. (1990). A scheme for predicting layer clouds and their water content in a general circulation model. *Q.J Royal Met. Soc.*, 116(492), 435–460. <https://doi.org/10.1002/qj.49711649210>

Soto-Navarro, J., Jordá, G., Amores, A., Cabos, W., Somot, S., Sevault, F., Macías, D., Djurdjevic, V., Sannino, G., Li, L., & Sein, D. (2020). Evolution of Mediterranean Sea water properties under climate change scenarios in the Med-CORDEX ensemble. *Clim Dyn*, 54(3–4), 2135–2165. <https://doi.org/10.1007/s00382-019-05105-4>

Stevens, B., Fiedler, S., Kinne, S., Peters, K., Rast, S., Müsse, J., Smith, S. J., & Mauritzen, T. (2017). MACv2-SP: a parameterization of anthropogenic aerosol optical properties and an associated



Twomey effect for use in CMIP6. *Geosci. Model Dev.*, 10(1), 433–452. <https://doi.org/10.5194/gmd-10-433-2017>

Strandberg, G., Bärring, L., Hansson, U., Jansson, C., Jones, C., Kjellström, E., Kupiainen, M., Nikulin, G., Samuelsson, P., & Ullerstig, A. (2015). *CORDEX scenarios for Europe from the Rossby Centre regional climate model RCA4*.

Szopa, S., Balkanski, Y., Schulz, M., Bekki, S., Cugnet, D., Fortems-Cheiney, A., Turquety, S., Cozic, A., Déandreibs, C., Hauglustaine, D., Idelkadi, A., Lathière, J., Lefevre, F., Marchand, M., Vuolo, R., Yan, N., & Dufresne, J.-L. (2013). Aerosol and ozone changes as forcing for climate evolution between 1850 and 2100. *Climate Dynamics*, 40(9–10), 2223–2250. <https://doi.org/10.1007/s00382-012-1408-y>

Tanré, D., J. F. Geleyn, & J.M. Slingo. (2000). *First results of the introduction of an advanced aerosol-radiation interaction in the ECMWF low resolution global model*, in *Aerosols and their Climatic Effects*, H.E. Gerber and A. Deepak, eds., A. Deepak Publishing, Hampton, Va, USA, 133–177.

Tegen, I., Hollrig, P., Chin, M., Fung, I., Jacob, D., & Penner, J. (1997a). Contribution of different aerosol species to the global aerosol extinction optical thickness: Estimates from model results. *Journal of Geophysical Research Atmospheres*, 102(20), 23895–23915. <https://doi.org/10.1029/97jd01864>

Tegen, I., Hollrig, P., Chin, M., Fung, I., Jacob, D., & Penner, J. (1997b). Contribution of different aerosol species to the global aerosol extinction optical thickness: Estimates from model results. *Journal of Geophysical Research Atmospheres*, 102(20), 23895–23915. <https://doi.org/10.1029/97jd01864>

Thatcher, M., & McGregor, J. L. (2009). Using a Scale-Selective Filter for Dynamical Downscaling with the Conformal Cubic Atmospheric Model. *Monthly Weather Review*, 137(6), 1742–1752. <https://doi.org/10.1175/2008mwr2599.1>

Thompson, G., Field, P. R., Rasmussen, R. M., & Hall, W. D. (2008). Explicit Forecasts of Winter Precipitation Using an Improved Bulk Microphysics Scheme. Part II: Implementation of a New Snow Parameterization. *Monthly Weather Review*, 136(12), 5095–5115. <https://doi.org/10.1175/2008mwr2387.1>

Tiedtke, M. (1989). A Comprehensive Mass Flux Scheme for Cumulus Parameterization in Large-Scale Models. *Mon. Wea. Rev.*, 117(8), 1779–1800. [https://doi.org/10.1175/1520-0493\(1989\)117<1779:acmfsp>2.0.co;2](https://doi.org/10.1175/1520-0493(1989)117<1779:acmfsp>2.0.co;2)

Tiedtke, M. (1996). An Extension of Cloud-Radiation Parameterization in the ECMWF Model: The Representation of Subgrid-Scale Variations of Optical Depth. *Mon. Wea. Rev.*, 124(4), 745–750. [https://doi.org/10.1175/1520-0493\(1996\)124<0745:aeocrp>2.0.co;2](https://doi.org/10.1175/1520-0493(1996)124<0745:aeocrp>2.0.co;2)

Top, S., Kotova, L., Cruz, L. D., Aniskevich, S., Bobylev, L., Troch, R. D., Gnatiuk, N., Gobin, A., Hamdi, R., Kriegsmann, A., Remedio, A. R., Sakalli, A., Vyver, H. V. D., Schaeybroeck, B. V., Zandersons, V., Maeyer, P. D., Termonia, P., & Caluwaerts, S. (2021). Evaluation of regional climate models ALARO-0 and REMO2015 at 0.22° resolution over the CORDEX Central Asia domain. *Geosci. Model Dev.*, 14(3), 1267–1293. <https://doi.org/10.5194/gmd-14-1267-2021>

Tucker S, M. J., Kendon E, Buonomo E, Jones R. (2018). *The UKCP18 12km RCM: PPE ensemble. Description and evaluation. In preparation.*



Turuncoglu, U. U. (2019). Toward modular in situ visualization in Earth system models: The regional modeling system RegESM 1.1. *Geosci. Model Dev.*, 12(1), 233–259. <https://doi.org/10.5194/gmd-12-233-2019>

V, D., & B, R. (2010). *Development of the EBU-POM coupled regional climate model and results from climate change experiments, in Advances in Environmental Modeling and Measurements*, Eds. Mihajlovic T. D. and Lalic B, Nova Publishers, pp. 23-32, ISBN: 978-1-60876-599-7.

Vadsaria, T., Li, L., Ramstein, G., & Dutay, J.-C. (2019). *Development of a sequential tool, LMDZ-NEMO-med-V1, to conduct global to regional past climate simulation for the Mediterranean basin: An Early Holocene case study*. <https://doi.org/10.5194/gmd-2019-196>

Valcke, S. (2013). The OASIS3 coupler: A European climate modelling community software. *Geosci. Model Dev.*, 6(2), 373–388. <https://doi.org/10.5194/gmd-6-373-2013>

Verseghy, D. L., McFarlane, N. A., & Lazare, M. (1993). Class—A Canadian land surface scheme for GCMS, II. Vegetation model and coupled runs. *Int. J. Climatol.*, 13(4), 347–370. <https://doi.org/10.1002/joc.3370130402>

Virgilio, G. D., Evans, J. P., Luca, A. D., Olson, R., Argüeso, D., Kala, J., Andrys, J., Hoffmann, P., Katzfey, J. J., & Rockel, B. (2019). Evaluating reanalysis-driven CORDEX regional climate models over Australia: Model performance and errors. *Clim Dyn*, 53(5–6), 2985–3005. <https://doi.org/10.1007/s00382-019-04672-w>

Vuuren, D. P. van, Edmonds, J., Kainuma, M., Riahi, K., Thomson, A., Hibbard, K., Hurtt, G. C., Kram, T., Krey, V., Lamarque, J.-F., Masui, T., Meinshausen, M., Nakicenovic, N., Smith, S. J., & Rose, S. K. (2011). The representative concentration pathways: An overview. *Climatic Change*, 109(1–2), 5–31. <https://doi.org/10.1007/s10584-011-0148-z>

Walters, D., Baran, A. J., Boutle, I., Brooks, M., Earnshaw, P., Edwards, J., Furtado, K., Hill, P., Lock, A., Manners, J., Morcrette, C., Mulcahy, J., Sanchez, C., Smith, C., Stratton, R., Tennant, W., Tomassini, L., Van Weverberg, K., Vosper, S., ... Zerroukat, M. (2019). The Met Office Unified Model Global Atmosphere 7.0/7.1 and JULES Global Land 7.0 configurations. *Geoscientific Model Development*, 12(5), 1909–1963. <https://doi.org/10.5194/gmd-12-1909-2019>

Zeng, X., Zhao, M., & Dickinson, R. E. (1998). Intercomparison of Bulk Aerodynamic Algorithms for the Computation of Sea Surface Fluxes Using TOGA COARE and TAO Data. *J. Climate*, 11(10), 2628–2644. [https://doi.org/10.1175/1520-0442\(1998\)011<2628:iobaaf>2.0.co;2](https://doi.org/10.1175/1520-0442(1998)011<2628:iobaaf>2.0.co;2)

Zhao, Q., Black, T. L., & Baldwin, M. E. (1997). Implementation of the Cloud Prediction Scheme in the Eta Model at NCEP. *Wea. Forecasting*, 12(3), 697–712. [https://doi.org/10.1175/1520-0434\(1997\)012<0697:iotcps>2.0.co;2](https://doi.org/10.1175/1520-0434(1997)012<0697:iotcps>2.0.co;2)

Zittis, G., & Hadjinicolaou, P. (2016). The effect of radiation parameterization schemes on surface temperature in regional climate simulations over the MENA-CORDEX domain. *Int. J. Climatol.*, 37(10), 3847–3862. <https://doi.org/10.1002/joc.4959>

Zittis, George, Hadjinicolaou, P., & Lelieveld, J. (2014). Comparison of WRF Model Physics Parameterizations over the MENA-CORDEX Domain. *AJCC*, 03(05), 490–511. <https://doi.org/10.4236/ajcc.2014.35042>